Maria Sklodowska-Curie Actions (MSCA)
Innovative Training Networks (ITN)
H2020-MSCA-ITN-2018
Grant number 813137

Project number 813137

URBASIS-EU

New challenges for Urban Engineering Seismology

DELIVERABLE

Work Package : WP3
Number: D3.6 – State-of-the-art fragility curves of typical RC and masonry structures considering SFSI and aging effects

Authors: **Amendola, Chiara** (AUTH)
Co-Authors: Pitilakis, Dimitris (AUTH)

Reviewers	Helen Crowley
Approval	Management Board
Status	Final Version
Dissemination level	Public
Delivery deadline	31.10.2020
Submission date	12.01.2021
Intranet path	https://urbasis-eu.osug.fr/Scientific-Reports-157

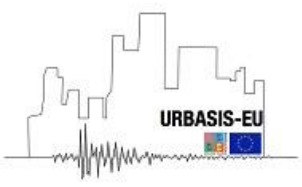

Maria Sklodowska-Curie Actions (MSCA)
Innovative Training Networks (ITN)
H2020-MSCA-ITN-2018
Grant number 813137

D3.6: State-of-the-art fragility curves of typical RC and masonry structures considering SFSI and aging effects

Vulnerability assessment is commonly carried out considering fixed-base structures, i.e. neglecting the interaction between the soil, foundation and structure (SFSI) as well as the impact of progressive deterioration due to various time-variant mechanisms. In the past decades, many research efforts were dedicated to highlight how SFSI and aging can modify the response of a structure subjected to earthquakes, and consequently have effects on fragility and vulnerability assessment. In this light, the up-to-date literature proves that neglecting those effects may lead to inaccurate fragility and loss estimates, which constitute fundamental components in the framework of risk assessment. To understand the current challenges related to the aforementioned effects, this deliverable reviews the state-of-the-art of fragility curves considering SFSI and aging effects. In the following, after a short theoretical background on fragility curves (Section 1) the effects of SFSI (Section 2) and aging (Section 3) on fragility curves are outlined.

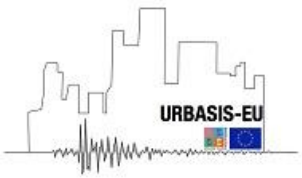

1 Seismic fragility analysis

In the last years, fragility curves have emerged as fundamental support tools for decision-makers and stakeholders to identify the potential seismic risk and the consequences in pre- and post-earthquake management. The fragility can be defined as the conditional probability of exceeding a predefined limit state given the intensity measure (IM):

$$P[D > C_{LS}|IM] = \phi\left[\frac{lnIM - ln\mu_{IM}}{\beta_{IM}}\right] \quad (1)$$

where D denotes the structural demand and C_{LS} is the capacity of the structure associated with different prescribed limit states LS. This probability, as reported in Eq. (1), can be expressed as a standard normal cumulative function Φ with respect to the IM at the performance point (see Figure 1). Where μ_{IM} is the median threshold value of the earthquake parameter IM required to cause the achievement of the performance level, β_{IM} is the total log-standard deviation.

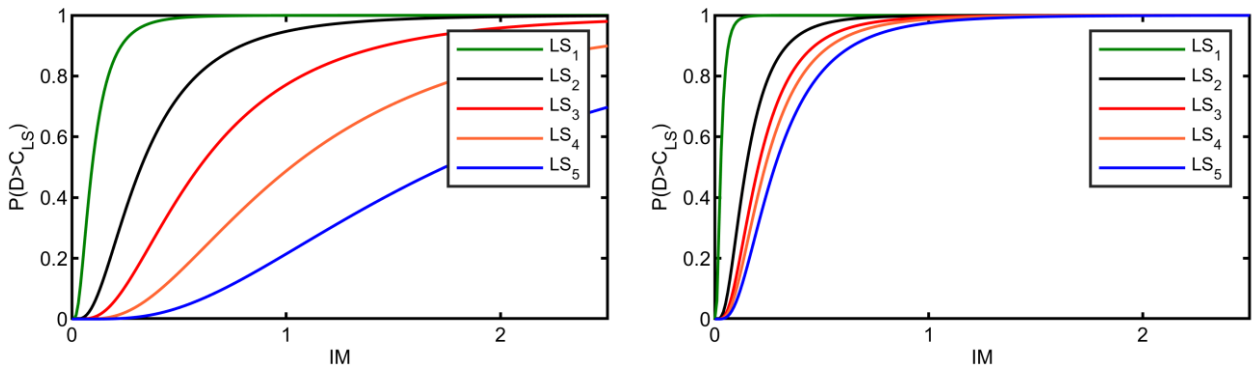

Figure 1 Fragility functions for low-code reinforced concrete (a) medium-rise frame structures and (b) medium-rise dual-system structures considering different limit states: LS_1=Slight, LS_2=Moderate, LS_3=Substantial to heavy, LS_4=Very Heavy, LS_5=Complete (Kappos et al., 2003)[57].

The ground motion intensity measure, IM, represents the earthquake-induced ground shaking. Several studies addressed different IM for fragility's computation in the last decades (Luco and Cornell, 2007 [71]; Porter et al., 2007 [90]), because there are signal

characteristics that influence the structural response but are not fully represented by IM (Baltzopoulos et al., 2017 [6]). In this regard, IM should be chosen to reach desired properties such as sufficiency, efficiency (Ebrahimian et al., 2015 [37]) scaling robustness (Tothong and Luco, 2007 [115]) and hazard computability (Giovenale et al., 2004 [45]), further explained in the following. An intensity measure is sufficient if the probability distribution of the conditional structural response to IM, i.e. P[D|IM] does not depend on any earthquake characteristics outside of IM. On the other hand, an intensity measure is efficient if leads to relatively small variability of demand measure (D) given IM. Consequently, one intensity measure is more efficient than another if, with the same accuracy in estimating the demand set, the intensity level is such that the demand distribution P[D|IM] estimate is obtained with a smaller number of analyses. Recent studies have also shown a relation between these two IM properties, in particular Bradley et al. (2010) [14] found that the more efficient is the IM, the higher is the sufficiency.

Scaling robustness of the chosen IM is another important assumption, i.e. the practice of scaling the accelerogram is legitimate if the structural response corresponding to a given level of IM is the same as what would get by applying a ground motion recorded with the same IM (Iervolino and Cornell, 2005 [48]). Finally, IM should be efficient for seismic hazard computability. For example, hazard maps are available for PGA or spectral acceleration at different discrete periods (INGV [49]; USGS [117]); nonetheless, other IM such as the commonly used spectral acceleration in correspondence of the first period of the structure require more information and effort for their determination.

During the years different intensity measure types have been used, which can be classified into two main categories: observational IM types and instrumental IM types (Pitilakis et a., 2014 [89]). With regard to the first categories, different IM have been largely used to characterize the ground shaking intensity, such as Mercalli-Cancani-Sieberg Intensity Scale (MCS), Modified Mercalli Intensity Scale (MMI), Medvedev-Sponheuer-Karnik Intensity Scale (MSK81), European Macroseismic Scale (EMS98). As reported in Figure 1, the peak ground acceleration PGA is the most commonly used instrumental intensity measure accounting for the 38% of the IM for the fragility studies addressed in Pitilakis et al. (2014) [89].

This is followed by the spectral displacement at the natural period of the structure $S_d(T)$ (Castaldo et al., 2017 [19]; Castaldo and Alfano, 2020 [18]) or at the anelastic period

S_d(TLS), accounting for the 23 and 15% respectively. Different authors have brought forth the use of the spectral acceleration at the fundamental vibration period of the structure S_a(T).

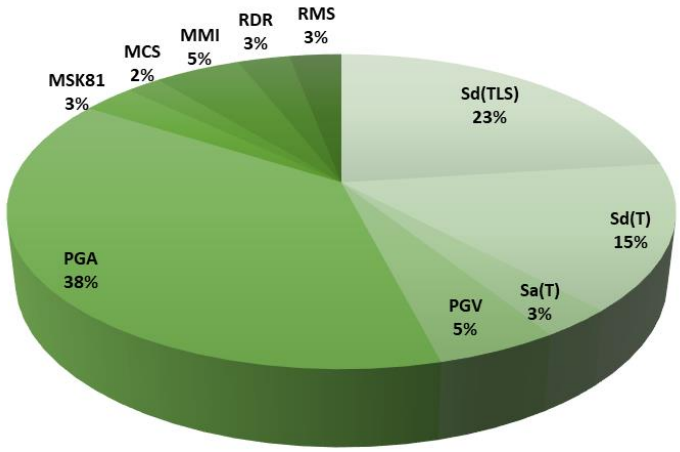

Figure 2 Pie chart presenting the different percentages of intensity measures commonly used to develop fragility function for reinforced concrete buildings as reported in Pitilakis et al. (2014) [89].

The reason why PGA has been largely used in the past decades is because hazard models, and more specifically Ground motion prediction equations, were typically developed in terms of PGA (Sabetta and Pugliese, 1987 [101]; Bindi et al., 2011 [11]). However, PGA is more suitable for short period structures under low levels of intensity (Lagomarsino and Cattari, 2015 [68]). On the other hand, S_a(T) is generally considered and has shown to be more efficient than PGA and sufficient in several situations (Shome et al., 1998 [107]).

As a matter of fact, an elastic single degree of freedom system (SDOF) subjected to a different number of records characterized by the same S_a(T=oscillator period) will always exhibit the same maximum response. For this reason, the spectral acceleration S_a(T) is a good predictor of the response of an elastic multi-degree of freedom system (MDOF) dominated by the first mode of vibration. This is also true for the assessment of inelastic structures for the “equal displacement rule” (Vidic et al., 1994 [122]). A series of effective research attempts have also been made on more suitable IM for predicting the structural performance, such as the average spectral response acceleration, i.e., the sum of the natural logarithm of spectral acceleration values computed over a range of T values (Bianchini et al., 2009 [10]; Eads et al., 2013 [36]) or vector-valued IM (Baker and Cornell, 2006 [4]; Kohrangi and Vamvatsikos, 2018 [65]).

During the years different analytical and experimental data have been used to identify C_{LS}, i.e. the structural capacity associated with the performance level. Capacity is generally assumed to be a deterministic value (Bakalis and Vamvatsikos, 2018 [2]), and in such case, the identification at different limit states can be carried out by means of static non-linear analysis. In alternative the capacity can be identified directly from the results of non-linear dynamic analysis, in such case, it will be a random variable with its own distribution, usually lognormal, independent from the value of seismic intensity.

1.1 Methods for fragility computation

The fragility analysis of concrete structure, as well as masonry structures, can be performed by means of empirical, analytical and hybrid methods (Calvi et al., [17]).

1.1.1 Empirical methods

The development of fragility curves can be carried out based on judgmental and field observations (Figure 3) (Sabetta et al., 1998 [102]; Rossetto and Elnashai, 2003 [99]). In this case, fragility functions are expressed with respect to IM such as PGA or Sa(T) which are converted from the observed macroseismic intensity.

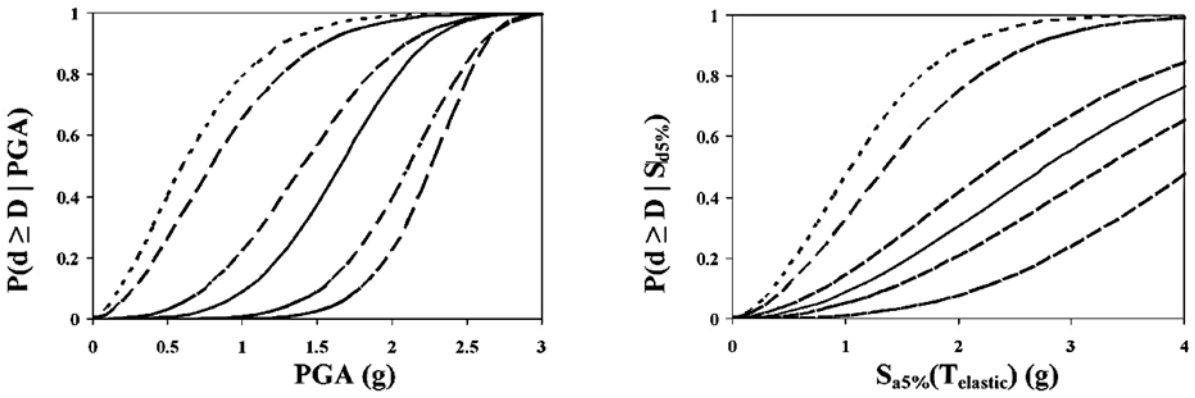

(a) (b)

Figure 3 Empirical vulnerability curves generated for (a) PGA and (b) Sa(T) for reinforced concrete building populations derived based on a data bank of 99 post-earthquake damage distributions observed in 19 earthquakes and concerning a total of 340 000 RC structures from the study of Rossetto and Elnashai (2003) [99].

These methods, being based on post-earthquake field investigations, are generally considered the most reliable and with less uncertainties, thus, can capture the real structural response to different earthquake scenarios. However, such fragility curves are strictly site- and structure-specific, and not replicable or usable for different scenarios. Moreover, they are generally limited to a small range of intensity measures. Furthermore, fragility curves derived from engineering judgment may not be reliable, because the opinions of a few experts may dominate the whole results.

1.1.2 Analytical methods

The lack of empirical data (Silva et al., 2019 [109]) at high intensity measure levels and the rapid development of computational tools has led to the analytical computation of fragility curves (D'Ayala et al., 2014 [30]). Analytical fragility curves are based on the estimation of damage distributions through the numerical analysis of structural models subjected to seismic loading. The first step in the fragility computation is to obtain, by numerical simulation, a link between the structural response and the seismic intensity measurement in the D-IM domain. Then, the analysis results will be a sample of points in terms of structural response, characterized by a distribution P[D|IM].

Analytical fragility functions can be developed using a variety of methods such as elastic spectral analysis, non-linear static analysis and nonlinear time history analysis. Despite being one of the most computationally expensive methods, the latter method of analysis is the most reliable one for generating fragility curves (Shinozuka et al., 2000 [106]) being able to catch the real response of structures subjected to seismic loading. Although, the actual application of the non-linear time history analysis further varies depending on the numerical simulation used when subjecting the structure to different records.

One of the simplest but not least time-consuming methods for generating fragility curves is the incremental dynamic analysis (IDA) (Vamvatsikos and Cornell, 2002 [118], Vamvatsikos et al., 2003 [119]). This kind of analysis arises from the need to characterize the fragility of the structure for high IM values. Indeed, it is well known that the increase in seismic intensity corresponds to earthquakes with a greater return period, i.e. rare or not

easily observable (D'Ayala et al., 2014 [30]). For this reason, IDA plans to scale records to find the desired IM value. The so-called IDA curves are then constructed by interpolating the resulting D-IM discrete pairs, as shown in Figure 4.

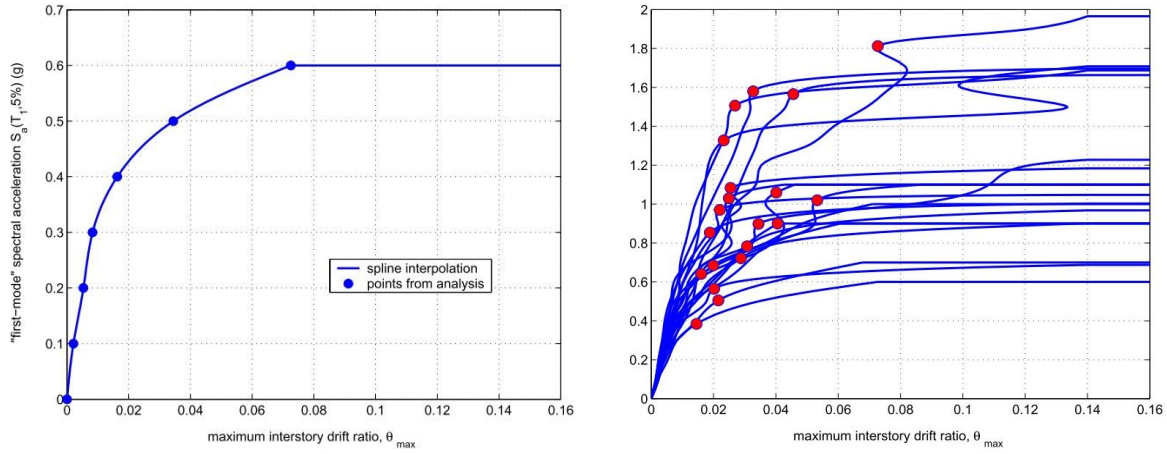

(a) (b)

Figure 4 (a) IDA curve resulting from spline interpolation of dynamic analysis results for a single record (blue dot points) and (b) 20 different records, including the associated limit-state capacity for collapse prevention limit state (red dot points) (Vamvatsikos et al., 2003 [119]).

Even though many researchers pointed out how excessive scaling can lead to remarkable bias in the dynamic response (Baker and Cornell, 2006 [4]; Lin et al., 2013a,b [69][70]). As an alternative, a multi-stripe analysis (MSA) (Jalayer and Cornell, 2003 [51]) can be performed by selecting multiple sets of records, each of which is used at a specific IM level spanning the IM domain. As suggested by different authors (Jalayer et al., 2017 [53]) it's desirable to perform non-linear analyses using unscaled records. In this regard, cloud analysis (CA) (Jalayer et al., 2015 [52]) is becoming widespread, selecting different records spanning the IM domain without the need for any scaling procedure.

That being said, analytical derivation of fragility curves typically involves fitting a parametric probability model to the results of dynamic analysis. Generally, a linear or piecewise-linear regression model is adopted to evaluate the dependent variable D as a function of the independent variable IM (see Figure 6) in the log-log scale. The most common form of linear regression is called least squares fitting mathematical tool for finding the best-

fitting line to a given set of points by minimizing the sum of the squares of the residuals (offsets) of the points from the line. The sum of the squares of the residuals is used instead of the offset absolute values since it allows the residuals to be treated as a continuous differentiable quantity. This mathematical model leads to a series of simplifying assumptions. The conditional standard deviation of D given IM does not depend on IM, consequently, the variation of D around the regression line will be the same across the IM values. This assumption of having constant dispersion is called homoskedasticity. It is worth mentioning that this limited assumption can be overcome by performing piece-wise linear regressions over different IM intervals. Further assumptions are the linear mean response versus IM in the logarithmic scale, and the lognormality of the response given IM (Jalayer et al., 2017 [53]). On the other hand, the dependence of the seismic demand D on the intensity measure IM in the linear scale can be easily expressed by a power-law model (Cornell et al., 2002 [26]) as reported in Eq. (2).

$$D = aIM^b \tag{2}$$

Within these simplifications, the coefficient of determination, i.e. the so-called R-square (R^2) can be evaluated since it provides information about how well the regression fits the data. It ranges between zero and one. Accordingly, as can be observed in Figure 5, the IM best predictor of D is the one corresponding to the R^2 values close to one (Ebrahimian et al., 2015 [37]).

Maria Sklodowska-Curie Actions (MSCA)
Innovative Training Networks (ITN)
H2020-MSCA-ITN-2018
Grant number 813137

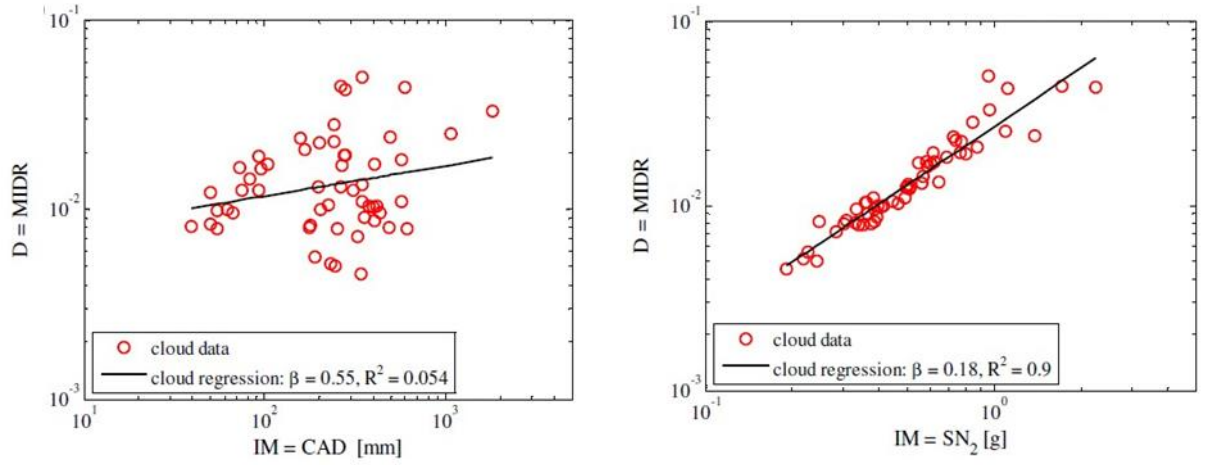

(a) (b)

Figure 5 Comparison of cloud regression using different intensity measures in case of (a) IM bad predictor of D and (b) IM good predictor of D (Ebrahimian et al., 2015 [37]).

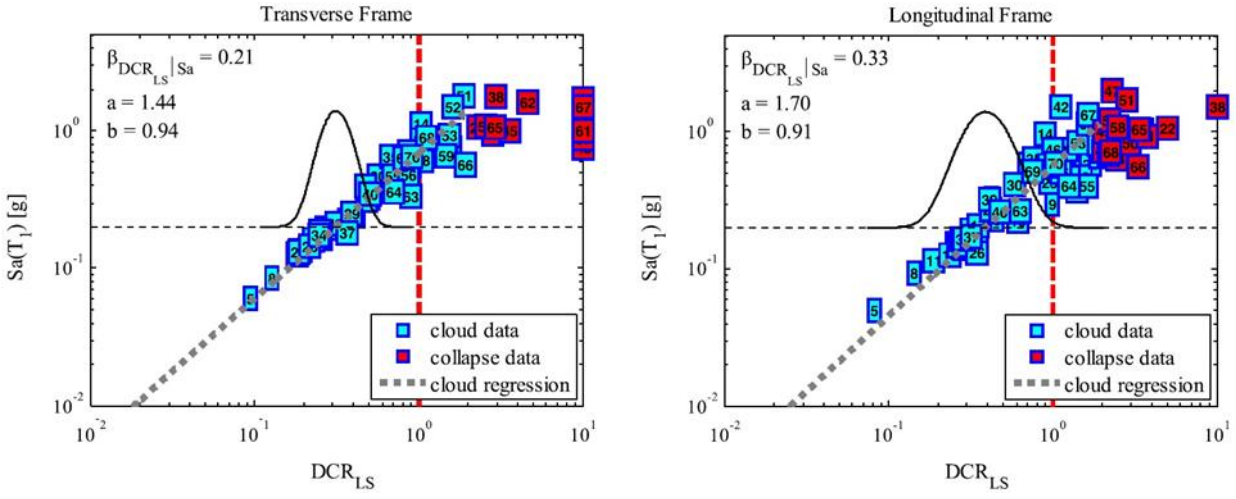

(a) (b)

Figure 6 Cloud Analysis data and regressions transverse and longitudinal frame, considering a large set of records as reported in Jalayer et al. (2017) [53].The slope and intercept of the logarithmic linear regression are reported on the left top side of each graph.

An inevitable consequence of such analytical methods is to deal with the so-called collapse cases (red square data points in Figure 6), i.e. the cases leading to structural collapse and/or reaching dynamic instability due to large deformations (Shome and Cornell, 2000 [108]). To formally consider the collapse cases, an improved fragility model is proposed in the literature in Jalayer et al. (2017) [53] mixing the simple regression (grey dashed line in Figure 6) in the log-log scale with logistic regression. As an alternative, different authors (see Crowley et al., 2017 [29]) propose to deal with collapse cases using a censored regression (Stafford, 2008 [111]) i.e. for example censoring the observations at 1.5 times the EDP associated to the complete damage state (Martin and Silva, 2020 [73]).

It is worth mentioning that in such cases applying a normal linear regression could lead to a biased model (Crowley et al., 2017 [29]). In order to overcome this issue, the maximum likelihood technique can be used calculating the fragility function parameters by varying the parameters until the likelihood function is maximized (Baker, 2015) [5].

One key aspect in the analytical fragility computation is the ground motion selection (Silva et al., 2019), since it provides the necessary link between seismic hazard and structural response (Lin et al., 2013a,b [69],[70]). In this regard, record selection should be carried out in order to reflect the expected dominant ground motion characteristics at each level of intensity measure. In particular, the parameter epsilon, i.e. the number of logarithmic standard deviations by which a given ground motion intensity measure value differs from the mean predicted value for a given magnitude and distance, is the record characteristic that mostly influences the distance between structural response and its mean value for a given intensity level (Baker and Cornell, 2006 [4]). Provided that, in the last years an increasing number of researchers (Iervolino and Cornell, 2005 [48]; Karapetrou et al., 2015 [60]) use epsilon as a proxy for spectral shape considerations. That being said, different records should be selected to match a target spectrum (Baker, 2011 [3]; Jayaram et al., 2011 [54]) and carefully chosen in order to reflect disaggregation (Bazzurro and Cornell., 1999 [7];Shome et al., 1998 [107]) of seismic hazard at each IM value.

1.1.3 Hybrid methods

In the framework of fragility analysis, to overcome the problems related to the aforementioned approaches such as the inadequate damage data from real earthquakes, the subjectivity of judgmental data and uncertainties associated with analytical procedures, in recent years have been proposed hybrid approaches which combine empirical data (appropriate for the area and structural typology considered) with analytical methods (Kappos et al., 2004,2006 [56],[58]; Kappos, 2016 [55]).

1.2 Uncertainties in fragility functions

Fragility functions are uncertain quantities, accounting for both aleatoric and epistemic uncertainties (Ellingwood and Kinali, 2009 [38]; Kiureghian and Ditlevsen, 2009 [64]). Aleatory uncertainty is associated with the intrinsic randomness of a phenomenon. On the other hand, the epistemic uncertainty is caused by a lack of knowledge. In the framework of more refined risk assessment is worthy to make such distinction since the lack of knowledge associated with the epistemic uncertainty can be reduced by intruding more data and using refined models. In general, the uncertainty of the fragility parameters is estimated through the standard deviation, β_{tot}, that describes the total variability associated with each fragility curve. This β_{tot} is modelled by the combination of the different variability sources (NIBS, 2004 [41]), assuming that they are stochastically independent and lognormally distributed random variables. The first source of uncertainty is associated with the definition of damage states. Moreover, capacity uncertainty is associated with the inherently modelling procedure as well as incomplete knowledge about structural properties, stiffness, ductility, and mass. Lastly, the record to record variability associated with the randomness of ground motions. Typical values of log standard deviations associated with the different sources can be found in NIBS (2004) [41], (i.e. for example the uncertainty in the damage-state threshold of the structural system is equal 0.4, for all structural damage states and building types and the variability in capacity properties of the model building is equal to 0.30 for Pre-Code buildings).

1.3 Fragility functions at urban scale

The fragility assessment presented so far can be applied at the site-building single case and can be further expanded to the urban scale. At the city scale, considering the high exposure concentration and moreover, the high level of complexity, the encouragement in the adoption of simplified models is fundamental to identify the most correct risk mitigation policies, both in short and long terms. Different methods of analysis for seismic risk at a large scale have been developed during the last years (D'Ayala et al., 2014 [30]; NIBS, 2004 [41]; Pitilakis et al., 2014 [89]). Most of these studies highlight how seismic vulnerability analysis at urban scale requires collecting information on the spatially distributed portfolio of structures and/or infrastructures. In the methodology proposed in Pitilakis et al. (2014) [89] the interactions between different components and systems are considered in the analysis, as they may lead to an increase in the global vulnerability and risk of the systems. To reduce considerably the computational effort involved in a fragility analysis on such a large scale it's convenient to classify buildings with similar characteristics as force resisting mechanism, height and code level, just to mention few. This classification, also known as taxonomy, is justified considering the structures with similar characteristics are more prone to experience similar behaviour when subjected to seismic forces. Different taxonomies have been provided during the last year for Europe as GEM taxonomy [30] and the one reported in Table 1 and USA (NIBS, 2004 [41]).

Table 1 SYNER-G taxonomy for buildings *in Pitilakis et al. (2014) [89].*

CATEGORY	**SUB-CATEGORY**
Force Resisting Mechanism (FRM1) • Moment Resisting Frame (MRF) • Structural Wall (W) • Flat Slab (FS) • Bearing Walls (BW) • Precast (P) • Confined Masonry (CM)	**Force Resisting Mechanism (FRM2)** • Embedded beams (EB) • Emergent beams (EGB)
FRM Material (FRMM1) • Concrete (C) • Masonry (M)	**FRM Material (FRMM2)** • Reinforced Concrete (RC) • Unreinforced Masonry (URM) • Reinforced Masonry (RM)

	• High strength concrete (>50MPa) (HSC) • Average strength concrete (20-50 MPa) (ASC) • Low strength concrete (<20 MPa) (LSC) • Fired brick (FB) • Hollow clay tile (HC) • Stone (S) • High yield strength reinforcing bars (>300MPa) (HY) • Low yield strength reinforcing bars (<300MPa) (LY) • Classification of reinforcing bars based on EC2 (A,B,C) • Lime mortar (LM) • Cement mortar (CM) • Mud mortar (MM) • Smooth rebars (SB) • Non-smooth rebars • Concrete Masonry Unit (CMU) • Autoclaved Aerated Concrete (AAC) • High % of voids (H%) • Low % of voids (L%) • Regular Cut (Rc) • Rubble (Ru)
Plan (P) • Regular (R) • Irregular (IR)	
Elevation (E) • Regular geometry (R) • Irregular geometry (IR) Cladding	
Cladding (C) • Regular infill vertically (RI) • Irregular infill vertically (IRI) • Bare (B)	**Cladding Characteristics (CM)** • Fired brick masonry (FB) • High % voids (H%) • Low % voids (L%)

	• Autoclaved Aerated Concrete (AAC) • Precast concrete (PC) • Glazing (G) • Single layer of cladding (SL) • Double layer of cladding (DL) • Open first floor (Pilotis) (P) • Open upper floor (U)
Detailing (D) • Ductile (D) • Non-ductile (ND) • With tie rods/beams (WTB) • Without tie rods/beams (WoTB)	
Floor System (FS) • Rigid (R) • Flexible (F)	**Floor System Material (FSM)** • Reinforced concrete (RC) • Steel (S) • Timber (T)
Roof System (RS) • Peaked (P) • Flat (F) • Gable End Walls (G)	**Roof System Material (RSM)** • Timber (Ti) • Thatch (Th) • Corrugated Metal Sheet (CMS)
Height Level (HL) • Low-rise (1-3) (L) • Mid-rise (4-7) (M) • High-rise (8-19) (H) • Tall (20+)(Ta)	**Number of stories (NS)**
Code Level (CL) • None (NC) • Low (<0.1g) (LC) • Moderate (0.1-0.3g) (MC) • High (>0.3g) (HC)	

Maria Sklodowska-Curie Actions (MSCA)
Innovative Training Networks (ITN)
H2020-MSCA-ITN-2018
Grant number 813137

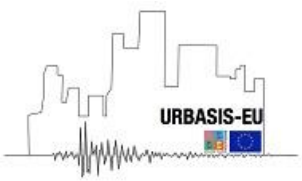

2 Soil-foundation-structure interaction

Despite the conventional design based on the fixed-base structure, the seismic response of a real building if the subsoil is soft, may be affected by the interaction among soil, foundation and structure. The modification of the dynamic behaviour of existing structures founded on soft soil with respect to the typical fixed-base assumption has been recognized by different authors in the past (Veletsos and Meek, 1974 [121]; Wolf, 1985 [123]; Paolucci, 1993 [82]) and more recently (de Silva, 2020 [32]; Piro et al., 2020 [86]). In deformable soil conditions, soil foundation structure interaction (SFSI hereafter) effects are expected, affecting the structural performance and modifying considerably the structure's seismic vulnerability compared to the reference case in which the structure is assumed as a fixed-base and no SFSI or site effects are taken into account (Rajeev and Tesfamariam, 2012 [91]). In this regard, in the framework of a more reliable risk assessment, the fragility curves need to be modified with the introduction of SFSI, in the case of compliant systems.

2.1 General notion on SFSI

If the subsoil is soft and the foundation depth is significant, the ‘kinematic interaction’ due to the relative soil-foundation stiffness may introduce a ‘filtering effect’ on the free-field motion (FFM) (Elsabee and Murray, 1977 [39]), which results in a different seismic action transmitted by the foundation to the structure also known as foundation input motion (FIM). For structures founded on shallow foundations, this filtering effect is often negligible (Kramer, 1996 [66]) and SFSI reduces to the so-called ‘inertial interaction’, where the absolute structural displacement is increased due to the subsoil compliance (Veletsos and Meek, 1974 [121]; Gazetas, 1983 [42]; Stewart et al., 1999a,b [112],[113]; Mylonakis and Gazetas, 2000 [77]). An increase of the fundamental period of the system is attributed to the inertial interaction (Maravas et al., 2014 [72]), due to deformability of the foundation soil. An increase of the overall damping is attributed to the energy dissipation mechanisms (wave radiation and hysteretic action) mobilized in vibrating SFSI systems (Mylonakis et al., 2006 [78]; Paolucci et al., 2013 [83]; Pitilakis et al., 2013 [87]). Moreover, in softer soil formations, the soil compliance can modify the structural performance leading to either beneficial or unfavourable effects, depending on the dynamic properties of the soil, the structure and the

characteristics (frequency content, amplitude, significant duration) of the input motion (Dutta et al., 2004 [35]; Sáez et al., 2011 [105]; Rajeev and Tesfamariam, 2012 [91]).

A first attempt to quantify the relevance of soil-foundation-structure interaction in the seismic demand can be performed by means of the structure-to-soil stiffness ratio $1/\sigma$ ($f\,h/V_S$) (NIST, 2012 [41]) in which f is the structural fixed-base fundamental frequency, h is the height of the structural gravity centre and V_S is the shear wave velocity of the underlying soil. If the structure-to-soil stiffness ratio $1/\sigma$ is greater than 0.1, the increase of the fundamental period and damping ratio is expected to be significant (Veletsos and Nair, 1974 [120]). In this regard, the influence of SFSI on seismic response of structures is often applied by modifying the fixed-base building period and the damping ratio considering the effects of foundation compliance (Maravas et al., 2014 [72]).

As already said, in seismic design procedures SFSI effects are generally neglected, mainly because of the expected seismic demand reduction associated with the period elongation and damping increase. It is worth clarifying that this is true only if the aforementioned increase in lateral natural period shifts to a region of the response spectrum which corresponds to a demand reduction (data points associated to the green arrow in Figure *7*). In the case of high-rise structures, i.e. for flexible systems, which fixed-base period lies in the long period region of the response spectrum, the spectral acceleration is generally expected to get reduced. On the other hand, as shown in Dutta et al. (2004) [35] in the case of low-rise structures SFSI may play a significant role in the increase of the seismic base shear force. Generally, the lateral fixed-base period of low-rise buildings being very small may lie within the initial sharply increasing zone of response spectrum (data points associated to the red arrow in Figure *7*). Hence, in such cases period elongation associated with SFSI may cause an increase in the spectral acceleration ordinate.

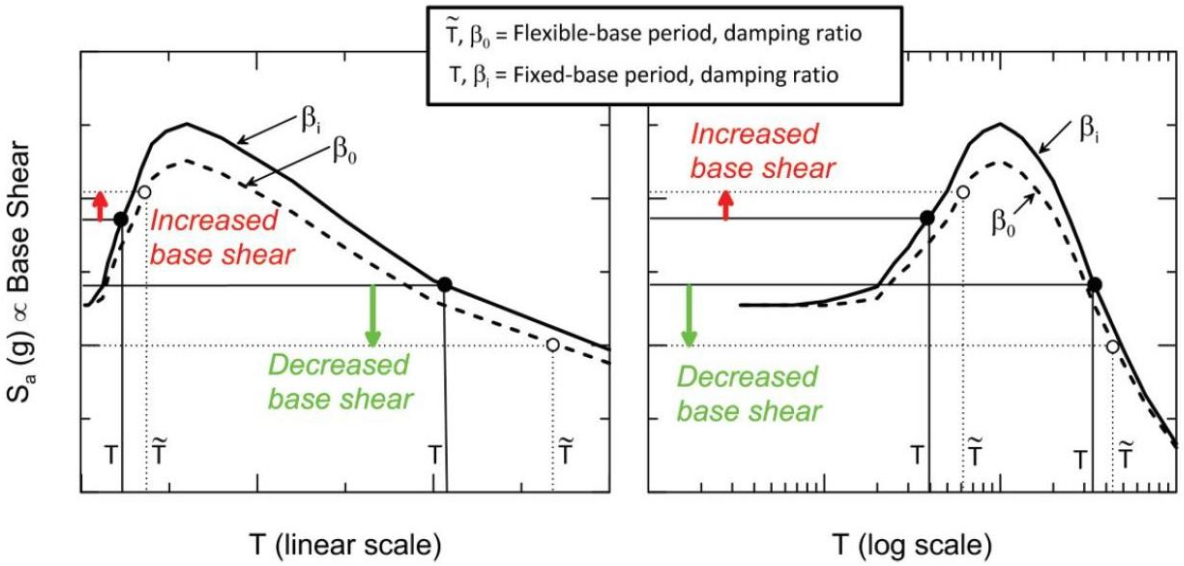

Figure 7 Illustration proposed in NIST (2012) [80] for inertial SFSI effects on spectral acceleration (base shear) associated with period lengthening and damping increase, considering the period (T) axis in (a) linear scale and (b) log scale.

On the other hand, period elongation is always associated with an increase in the displacement spectral ordinate. In fact, although SFSI tends to reduce the structural distortion, the foundation translation and rocking due to the soil compliance lead to an increase of the overall displacement (Karatzetzou et al., 2020 [61]).

2.2 Modelling approach of SFSI

In the up-to-date literature, the incorporation of SFSI in the analytical computation of fragility functions can be done by means of simplified approaches, based on the uncoupled 'substructure method', as well as refined complete SFSI models based on the 'direct method' (NIST, 2012 [80]). These approaches can be easily implemented in different software for generating fragility curves and have been proven to provide a reliable estimate of the seismic vulnerability of structures in soft soil conditions (Karapetrou et al., 2015 [60], Cavalieri et al., 2020 [22]).

Following the substructure approach, it is possible to decouple the interaction phenomena in two separate systems. Firstly, kinematic interaction is carried out by evaluating the FIM to be transmitted to the structure through the analysis of the massless foundation and structure. For inertial interaction analysis, the FIM is then applied to the structural system and inertial forces arise in the structure which in turn result in forces and moments at the foundation level. Following this simplified approach, kinematic effects (Kramer, 1996 [66]) can be introduced in the analysis by a frequency-dependent transfer function relating the free-field motion to the foundation input motion. For inertial interaction, in the most widespread simplified approach, also suggested by some international guidelines (BSSC, 2004 [16]), the structural model is placed on translational and rotational springs and dashpots simulating the frequency-dependent soil-foundation impedance functions. Analytical expressions for the real and complex impedance components available in the literature mostly refer to regular or irregular rigid massless foundations, more or less embedded in the soil (Pais and Kausel, 1988 [81]; Gazetas, 1991 [43]; NIST, 2012 [80]).

Over the last years, this approach has become one of the most widespread being the impedance functions easily implemented in modern software (Petridis and Pitilakis, 2020 [85]). For example, in the Open System for Earthquake Engineering Simulation (OpenSees) software (Mazzoni et al., 2006 [74]), such impedances can be implemented defining for each degree of freedom of the foundation elastic springs, modelled by means of zero-length elements. A more refined way to implement the inertial interaction in OpenSees can be done instead through Beam on Nonlinear Winkler Foundation (BNWF) model (Harden et al., 2005 [47]) shown in Figure 8(a). The update with respect to the previously mentioned technique is the possibility to account for soil-structure interaction phenomena using one-dimensional non-linear springs distributed along with the soil-foundation interface Figure 8(b). The ‘shallow generation’ command (Raychowdhury et al., 2008 [95]) automatically implements the BNWF model and consists of elastic beam-column elements that capture the structural footing behaviour with independent ‘zero-length’ soil elements that model the soil-footing behaviour.

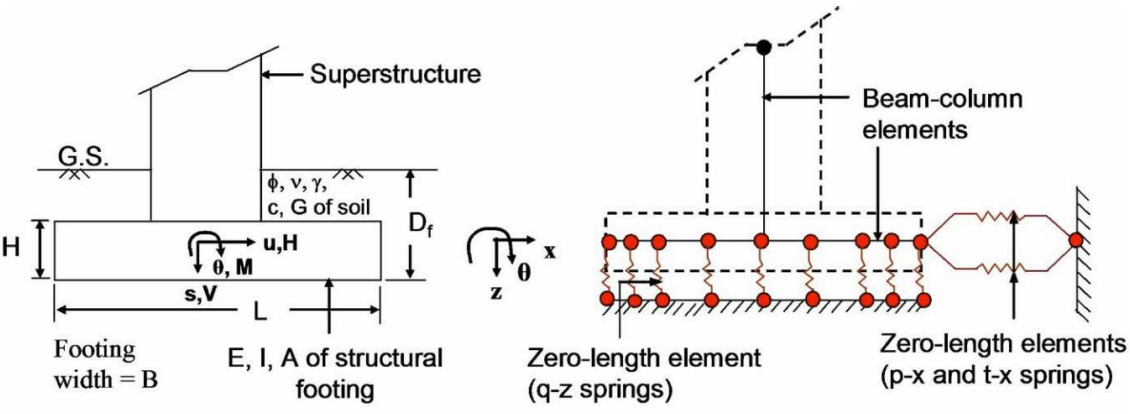

(a) (b)

Figure 8 Schematic illustration of beam-on-nonlinear-Winkler foundation (BNWF) (a) hypothesized foundation-superstructure system and (b) idealized model (Raychowdhury et al., 2008 [95]).

There has been a substantial increase in the adoption of this model among researchers since has been proved to correctly predict the experimentally observed behaviour of shallow foundation. However, taking into account the non-linearity may not be easily achievable by the substructure approach since it involves the application of the principle of superposition which applies only to linear systems (Kutanis and Elmas, 2001 [67]).

As an alternative, the direct approach can be adopted. Finite elements or finite difference complete models are generally justified only for high-value buildings (de Silva, 2020 [32]; Karatzetzou et al., 2020 [61]) due to the computational effort required for the analysis and the complications that may arise modelling the domain as well as the foundation-soil interface as shown in Figure 9. Specifically, the extension of the lateral boundaries should be checked thoroughly to correctly model the energy loss due to seismic wave propagation. Otherwise reflected waves may be generated leading generally to an overestimation of the amplification. Despite this, this method has the advantage of considering simultaneously both the inertial and the kinematic interaction effects and providing precious insights on the effects of non-linear soil behaviour (Pitilakis et al., 2014 [88]).

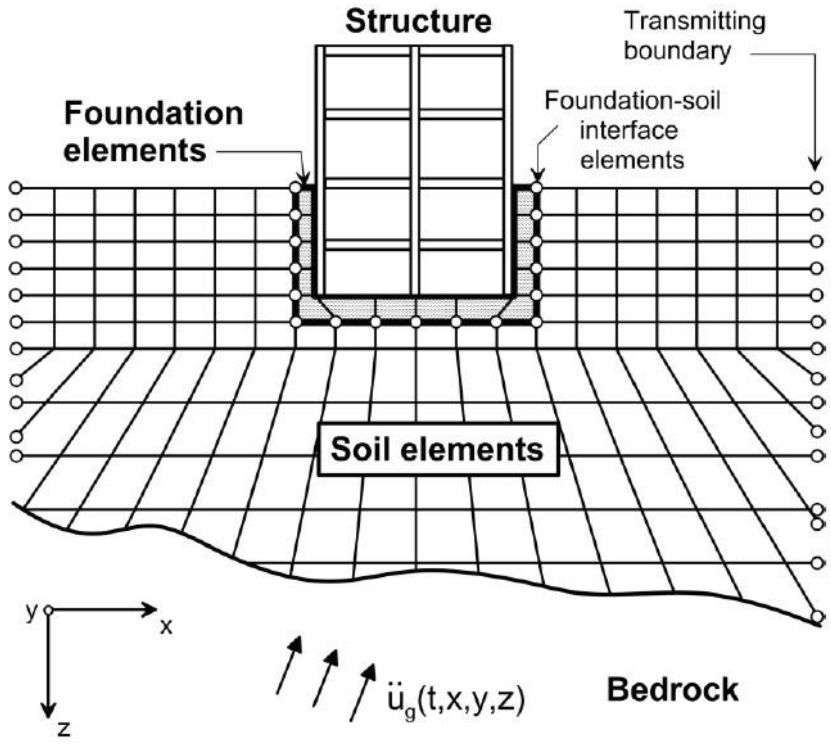

Figure 9 Schematic illustration of a direct analysis of soil-structure interaction using continuum modelling by finite elements proposed in NIST (2012) [80].

Different results may be obtained depending on the modelling used to assess the effects of the interaction (Karapetrou et al., 2013 [59]). In particular, the demand estimation evaluated when applying the direct method may be lower than the one assessed with the substructure approach (Tomeo et al., 2018 [114]).

2.3 Effects of SFSI on Vulnerability of structures

Nowadays only a few studies take into account the effects of SFSI in the vulnerability assessment of reinforced concrete and masonry structures. This is mainly because the incorporation of SFSI phenomena in the analysis, during the past years, has been generally considered beneficial reducing the seismic demand and consequently the corresponding structural damage of non-linear systems (Ciampoli and Pinto, 1995 [25]). More recently, it

has been recognized that SFSI might lead to non-negligible effects on the seismic demand as well as the seismic capacity of structures, modifying considerably the fragility functions.

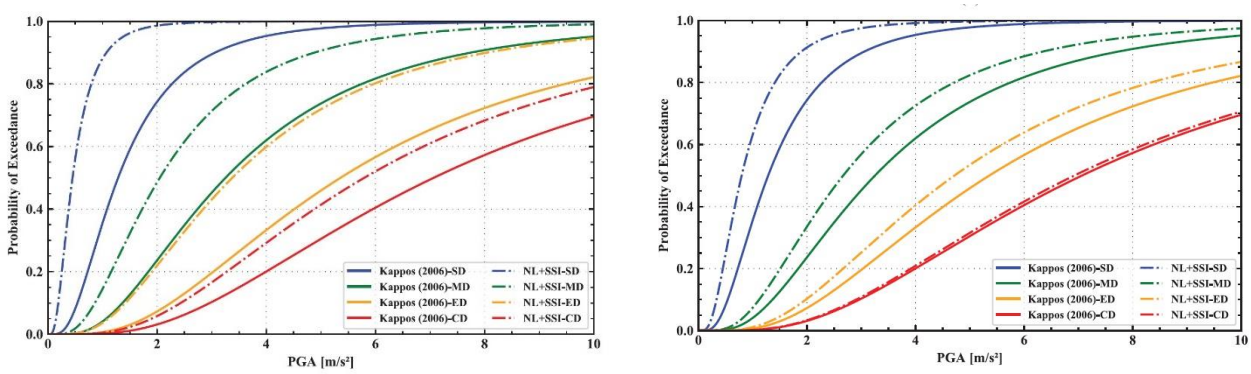

(a) (b)

Figure 10 Comparison between fragility curves considering SSI and NL soil behaviour effects for a 4-story infilled structure resting on compliant soil (dashed lines) with (a) Vs_{30}= 180 m/s and (b) Vs_{30}= 300 m/s and the reference fixed-base fragility curves from Kappos et al. (2006) [58] (continuous lines). Considering the following damage states: SD: slight damage, MD: moderate damage, ED: extensive damage, CD: complete damage, as reported in the study by Petridis and Pitilakis (2020) [85].

In particular, the consideration of site and SFSI effects may significantly change the behaviour of structures subjected to seismic loading, producing an important shift to the left of the fragility curves compared to the fixed-base case (i.e. for example Figure 10). Especially in the case of high-rise structures designed with low-code prescriptions (Karapetrou et al., 2015 [60]).

Besides, several analytical studies (Mitropoulou et al., 2016 [76]) once demonstrated the structural performance of high structures is considerably affected by the foundation system compared with the low and mid-rise buildings. Moreover, if the flexibility of the foundation is taken into account, an increase in the vulnerability of structural members of the lower stories of moment frame and dual system buildings is expected (Behnamfar and Banizadeh, 2016 [8]).

As stated before, SFSI effects decrease when the relative soil-structure stiffness increases. As a matter of fact, SFSI effects on vulnerability are shown to be more pronounced in the case of stiff structures resting on soft soil (corresponding to low σ values)

(Rajeev and Tesfamariam, 2012 [91]). Specifically, in such cases as well as for slender buildings in soft formation the damage index increases (Nakhaei and Ali Ghannad, 2008 [79]).

With a special focus on the influence of the uncertainties in soil properties, foundation, and ground motion characteristics Rajeev and Tesfamariam (2012) [91] investigated the effects of the SFSI on fragility curves. Performing dynamic analyses on low-code concrete frames including non-linear soil-foundation interaction through the BNWF model, they have shown that fragility curves including SFSI may differ from the fixed-base reference case. Among all the sources of uncertainties considered, the record-to-record variability was found the most influencing parameter dominating the structural response of the SFSI models.

The work proposed by Sáez et al. (2011) [105] provided further insight into the effects of different modelling approaches for SFSI on the seismic vulnerability assessment of buildings. They performed analyses applying the direct approach and two steps approach where only site effects are considered. In particular, the results of comparative dynamic analyses on these two systems highlighted that the consideration of site effects (even including the non-linear soil behaviour) modifying the imposed input motion to the fixed-base superstructure will lead to a conservative prediction of expected damages. This is mainly because the latter approach considers just the material damping in energy dissipation neglecting the radiation damping. The main findings of the authors once demonstrate that a general structural demand reduction is expected when dynamic SFSI effects are included. This reduction is mainly related to the combined effect of radiative damping, modification of vibrating modes and hysteretic soil dissipation due to its non-linear behaviour. Same evidence has been pointed out in Karapetrou et al. (2013) [59] who highlighted that the conservativeness of the sub-structuring method, which leads to higher vulnerability, may be attributed to the uncertainties in the evaluation of impedance functions.

To understand the role of non-linear dynamic SFSI on fragility computation, Karapetrou et al. (2015) [60] performed comparative analyses considering a coupled approach in which SFSI and site effects are considered inherently (assuming either linear and non-linear soli behaviour) and the uncoupled fixed-base model in which only site effects are considered. As reported in this study, when soil nonlinearity is considered, the coupled case of SFSI and site effects leads to a significant increase of the vulnerability compared to the fixed-base case where site effects are simply considered. This may be due to the

complex non-linear behaviour of the compliant soil which may introduce additional displacements to the structure, increasing i.e. the drift demands (Kramer, 1996 [66]). Furthermore, it was found that when the stratigraphy of the soil profile is taken into account, non-linear SFSI increases the vulnerability, since the layered soil medium may amplify the imposed input motion at the base of the structure in comparison to the homogeneous soil profile.

In order to investigate the importance and relevant contribution of site and SSI effects on the vulnerability assessment, Karapetrou et al. (2013) [59] retrieved fragility curves adopting sub-structure and direct SFSI models. The findings show that considering only the modification of the input motion in case of soft soil may lead to a slight increase in vulnerability compared to the case in which SFSI are taken into account. Within the same issue, recently Petridis and Pitilakis (2020) [85] found also that ground motion amplification leads to higher vulnerability than SFSI effects alone; this evidence is likely to be more pronounced for slight damage states due to the de-amplification phenomenon occurring for high IM values. In particular, the modification of PGA corresponding to 50% probability of exceeding the slight damage state of the actual SFSI systems (i.e. low-rise structure on soft soil V_S=180 m/s) is about 30–50% of the corresponding PGA for fixed-base structure. This percentage increases to 70% with reference to PGA for the fixed-base on soft soil condition, i.e. where SFSI on fragility curves are isolated.

The seismic assessment of masonry structures has attracted relatively little attention from researchers in the field of SFSI compared to reinforced concrete structures. The available studies show that the soil compliance can modify the structural performance leading to either beneficial or unfavourable effects. In particular, Fathi et al. (2020) [40] investigated the impact of SFSI on the out-of-plane behaviour of a historic masonry building revealing that SFSI has a significant decreasing effect on the spectral acceleration response and a remarkable increasing impact on the displacement response due to increasing of first mode vibration period. Later studies of Güllü and Jaf (2016) [46] assessed the effect of near-fault and far-fault earthquakes on a historical masonry mosque through 3D dynamic SFSI analysis. They found the influence of SFSI to the near and far-fault effects, increases amplitude and stresses, compared with the reference fixed-base results.

With a special focus on the role of SFSI on vulnerability assessment of masonry structures, Karatzetzou et al. (2015) [62] performed static non-linear analyses on the

masonry Neoclassical School in Rhodes, Greece. Main findings of the study revealed that SFSI and foundation flexibility may lead larger displacements and reduce by half the PGA that the structure is able to withstand. Despite these detrimental, SFSI and foundation flexibility may have a favourable effect on the structure safety, leading to a different collapse mechanism. It was shown that for the fixed-base model, collapse occurs simultaneously on all piers of the wall, whereas, in the compliant model, collapse of structural elements takes place sequentially.

More recently, in the study performed by de Silva (2020) [32] it is investigated and compared the site-specific seismic demand required to squat or slender masonry towers resting on stiff or soft soil performing dynamic analysis on 3D direct models. The results of the analyses once shown that SFSI effect can be either beneficial or detrimental, i.e. the period of the SFSI system may tend to be closer or further to the resonance of the free field soil layer. Moreover, it is shown that soil deformability enhances the bending demand and produces a not negligible permanent tilt in the towers leading to an increase of the system vulnerability.

Later studies of Cavalieri et al. (2020) [22] provided insights into the impact of adopting different SFSI of models of shallow foundations on the characterisation of fragility functions for the unreinforced masonry (URM). To this aim they modelled SFSI using two models according to the substructure approach, (i.e. one-dimensional frequency-independent model (1-D) and a Lumped-Parameter Model (LPM) accounting for frequency dependence of the impedance) and a third one that relies on the adoption of a nonlinear macro-element (ME). By performing non-linear time history analyses on such models, they found a non-negligible influence of SFSI on the fragility analysis only for stiffer buildings (Figure 11). The analysis results show that SFSI leads towards a less fragile response, in comparison to the fixed-base reference case (grey dashed curves in Figure 11). Furthermore, considering inelastic behaviour in the SFSI model (green continuous line in Figure 11) lead to smaller structural displacements and consequently to a lower vulnerability, even more pronounced for high levels of intensity measures.

It is rather clear that the literature review presented herein, i.e. available studies implementing SFSI in risk assessment are limited to the single building scale. Nevertheless, only few studies investigated thoroughly what is the role of SFSI on risk assessment at the urban scale (Michel and Guéguen, 2012 [75]; Karatzetzou et al., 2017 [63]; Riga et al.,

2017,2019 [97],[96]). In seismic risk assessment, large scale analyses are commonly carried out applying existing fragility curves (Smerzini and Pitilakis, 2018 [110]; De Risi et al., 2019 [31]). Including SFSI phenomena in the urban vulnerability assessment is considered a challenging task (Silva et al., 2019 [109]) since different approaches and methodologies are spread across scientific researchers. More specifically, the vulnerability of the SFSI system depends on the dynamic characteristics of the structures, soil conditions and ground motion, and thus will differ from the assessment of the same building resting on different site conditions.

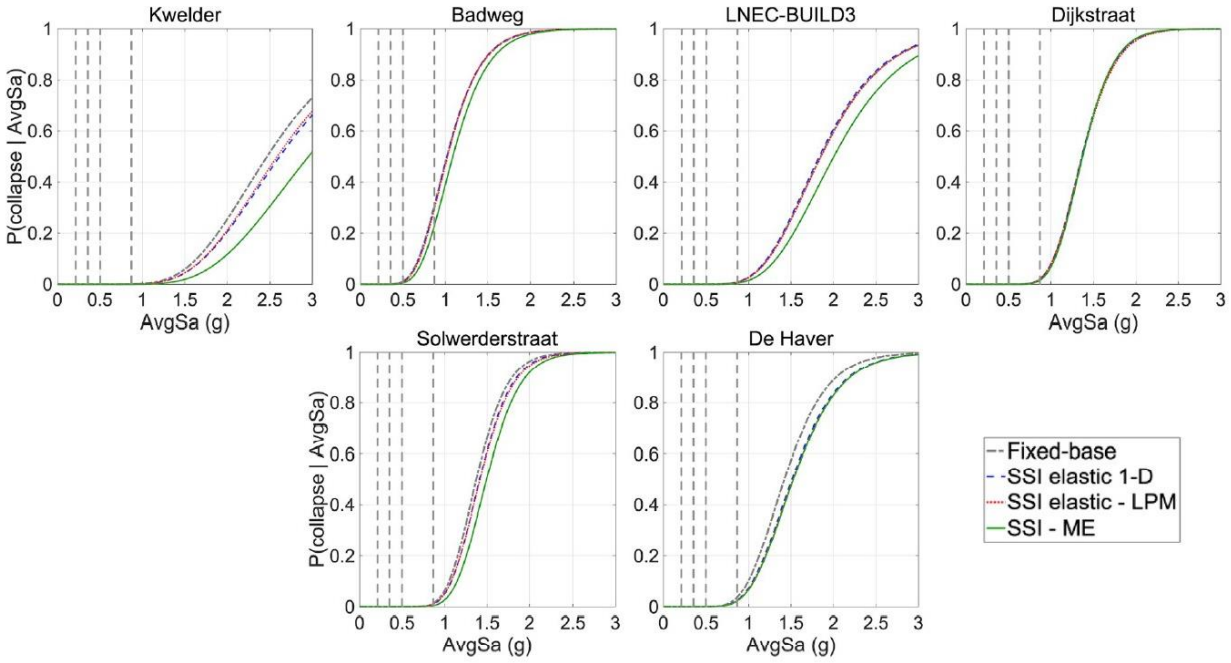

Figure 11 Comparison of the fragility curves proposed in Cavalieri et al. (2020) [22] for three SSI models and for different index buildings corresponding to various fixed-base periods (Kwelder T=0.08s, Badweg T=0.13s, LNEC-BUILD3 T=0.08s, Dijkstraat T=0.36s, Solwerderstraat T=0.3s, De Haver T=0.13s). The grey dashed vertical lines indicate the four considered levels of AvgSa: Tr 500, 2500, 10 and 100 years.

Most studies investigating the effects of soil-structure interaction in urban areas considered data recorded on monitored buildings (Michel and Guéguen, 2012 [75]) have been focused on the elongation of the fundamental period (Rovithis et al., 2017 [100]) and the evaluation of the damping ratio of the system with consequent modification of fragility

curves. The main findings reported in Michel and Guéguen (2012) [75] show that considering ambient vibration recordings in buildings would provide the actual dynamic behaviour of buildings under low strains and can be suitable for the prediction of slight damage states. The results of the analyses performed by Karatzetzou et al. (2017) [63] indicate that consideration of SFSI at an urban-scale may lead to higher seismic forces compared to the currently employed fixed-base approach.

An alternative to reduce the computational effort required by the urban scale vulnerability assessment could be the consideration of secondary factors, which increase or decrease the seismic vulnerability. To this aim, based on the work proposed by Petridis and Pitilakis (2020) [85] it is possible to modify the existing fragility curves for reinforced concrete buildings to introduce the influence of nonlinear SFSI, without the need to run individual building-to-building analyses. More specifically, the Authors propose to shift the existing fragility curves for fixed-base structures by multiplying the median value for each damage state with an appropriate modifier depending on both structure and soil parameters, as reported in the heat map of Figure 12.

This methodology can be implemented at an urban scale based on globally available data regarding the soil parameters, the foundation, and the building taxonomy, all necessary to define these fragility modifiers.

Maria Sklodowska-Curie Actions (MSCA)
Innovative Training Networks (ITN)
H2020-MSCA-ITN-2018
Grant number 813137

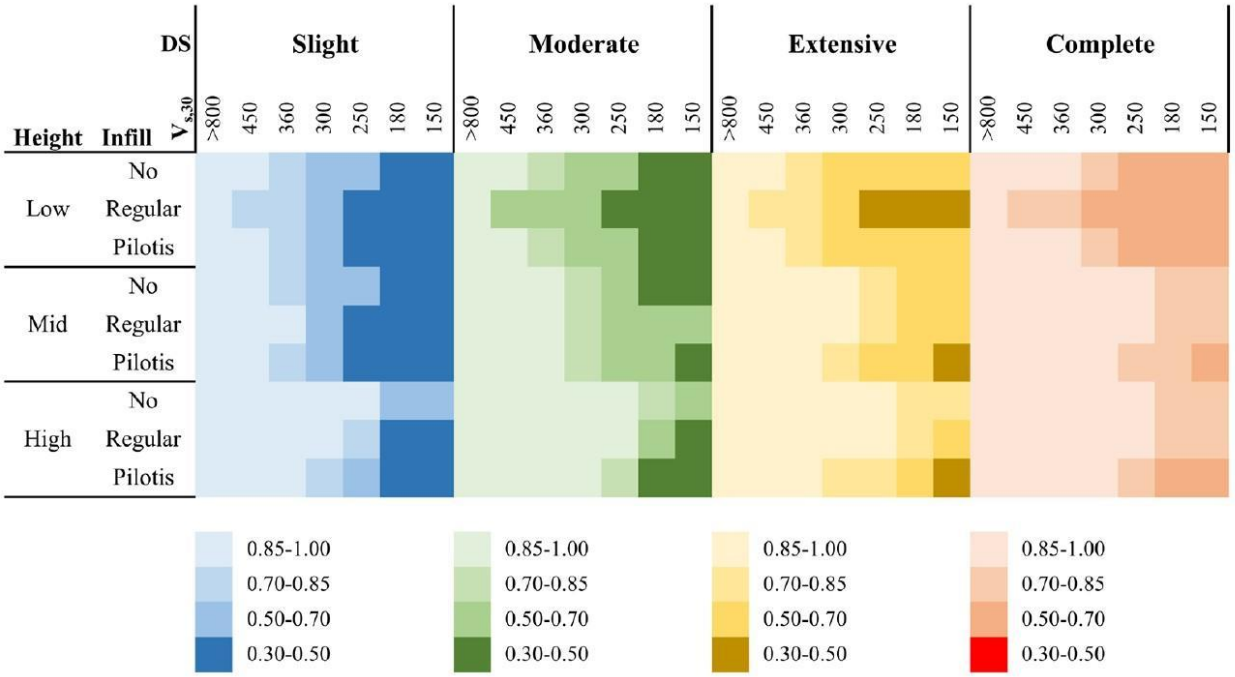

Figure 12 Heat map reported in Petridis and Pitilakis (2020) [85]: "Flexible-base on soil" to "Fixed-base on rock" ratios of median PGA to exceed each DS, described as fragility modifier (FM). The discretization is based on the height of the structure (low, medium, high), the infill type (no, regular, pilotis), the damage state (slight, moderate, extensive, complete) and the soil shear wave velocity. Darker color implies stronger influence of soil nonlinearity and SSI.

3 Aging effects

The up-to-date vulnerability assessment of existing buildings assumes that the mechanical properties of reinforced concrete, as well as masonry structures, remain constant over time. When an existing structure is assessed its material may be softer due to deterioration phenomena affecting progressively the building over time (Saetta et al., 2008 [104]; Castaldo et al., 2017 [21]). Recent studies on the topic have demonstrated that so-called aging effects worsen the mechanical properties of the building, depending on the type and location of the construction. In this light, especially when the concrete is exposed to an aggressive environment, mechanical degradation should be taken into account in the fragility computation in order to enhance the whole reliability of the risk assessment procedure.

3.1 General notions on Aging effects

The deterioration phenomena may be induced by different sources as a diffusive attack of environmental aggressive agents, such as chloride and sulfate ions, or by carbonation phenomenon, alkali-aggregate reaction, freeze-thaw cycles, etc. (Cosenza et al., 2008 [28]). The aging effect is mainly related to the corrosion of steel bars (Pitilakis et al., 2014 [88]) and it consists of a two-phase process: initiation and propagation phase (Tuutti, 1982 [116]). In normal conditions (basic environment, PH> about 13) steel is covered by a passive protective layer, impenetrable to external ions. As soon as the concentration of chlorides or carbon dioxides exceeds a critical value, the PH tends to decrease causing the destruction of the passive layer and consequently leading to the initiation of corrosion. The corrosive phenomena can be manifested with the simple appearance of rust spots on the covering or with cracks and spalling caused by the expansive action of the corrosion products (rust), finally resulting in significant structural damage.

Several experimental and analytical investigations showed the main effect of corrosion involves the reduction of the cross-sectional area of the reinforcing steel bars (Figure 13a). Moreover, the progressively concrete cracking may lead to a reduction of concrete strength, delamination and spalling of the concrete cover. Furthermore, the whole corrosion process may affect the steel-concrete bond strength and lead to the reduction of steel ultimate deformation during time as shown in Figure 13b (DuraCrete, 1998 [34]; Saetta

et al.,1999 [103]; Berto et al., 2009 [9]; Yalciner et al., 2012 [124]). Thus, on reinforced concrete structures, these phenomena may imply a significant loss of ductility due to high corrosion levels, decreasing the capacity to withstand the applied loads (Castaldo et al., 2017 [21]), as well as a shift to more brittle failure mechanisms is expected (Berto et al., 2009 [9]; Yalciner et al., 2012 [124]).

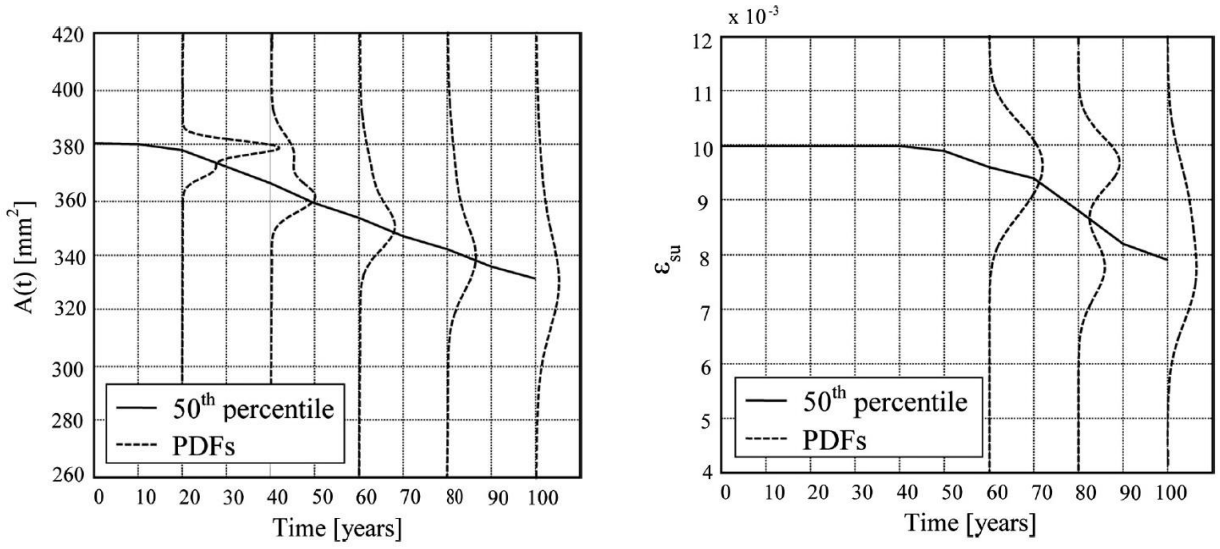

(a) (b)

Figure 13 Time evolution of both the 50th percentile value and bimodal PDFs related to (a) the cross sectional area of the reinforced stell A(t) and of (b) the ultimate deformation ε_{su} derived from MonteCarlo simulations of degradation models for material properties as reported in Castaldo et al. (2017) [21].

.

In the up-to-date seismic design procedures the above-described phenomena can be limited by prescribing the fulfilment of required levels of the quality of the materials and structural detailing. In particular, depending on the environmental exposure (humidity, temperature, carbon dioxide or chloride concentration) different threshold values are proposed in terms of concrete cover depth, water-cement ratio, amount and type of cement.

Much effort has been devoted lately to understanding that design to prevent aging effects cannot be limited to that simplified design-criteria. Aging effects should be carefully considered through analysis methods capable to include the global effects of local damage

phenomena on the overall performance of the structure in order to assess the time-variant structural safety (Biondini and Vergani, 2015 [12]).

3.2 Modelling approach of aging effects

The analysis of corroded RC and masonry structures incorporating aging effects and the progressive degradation can be performed employing finite-elements models including the effects of mechanical and environmental damage (Saetta et al.,1999 [103]; Coronelli and Gambarova, 2004 [27]; Biondini and Vergani, 2015 [12]). Several models have been proposed in literature aimed to quantify and account for the degradation process and the corresponding effects on RC structures. A summary of these models can be found in DuraCrete (1998) [34]. Any of the above-mentioned effects concerning the material deterioration of RC structures start with the beginning of reinforcement corrosion.

In this regard, one of the key aspects in the modelling of the degrading phenomenon is related to the correct estimation of the initiation time (T_{ini}) (Saetta et al.,1999 [103]). If among the various above mentioned aging processes, the chloride-induced corrosion is considered, the probabilistic model proposed by FIB-CEB Task Group 5.6 (2006) [23] can be adopted to evaluate the corrosion initiation time. In such a case, T_{ini} is mostly influenced by the steel bars cover and chloride surface concentration. In particular, increasing the steel bar cover T_{ini} tends to increase and on the contrary, tends to decrease increasing the superficial concentration of chlorides.

Moreover, the evolution over time of structural behaviour in terms of the geometry, material (Argyroudis et al., 2014 [1]) as well as bond properties (Coronelli and Gambarova, 2004 [27]) has to be considered in the model. In particular, the time-dependent loss of reinforcement cross-sectional area can be evaluated following the approach proposed by Ghosh and Padgett (2010) [44], the cracking and spalling of the cover concrete can be considered reducing the concrete cover strength following to the model proposed by Coronelli and Gambarova (2004) [27]. Finally, the loss of steel ductility can be considered through the reduction of the steel ultimate deformation using the model proposed by Rodriguez and Geocısa (2001) [98]. Furthermore, a nonlinear model able to describe the evolution of structural degradation over time is strongly required. In the framework of non-

linear modelling through a lumped plasticity approach, aging effects may be introduced in the model by modifying the constitutive relationships of the plastic hinges depending on the corrosion level (Saetta et al., 2008 [104]). Following this approach, Berto et al. (2009) [9] investigated the influence of rebars corrosion on the seismic response of RC structures. The main results of this study show the reduction of load-bearing capacity of the structure and, in several cases, also the shift of the failure mechanism from the ductile to the brittle type.

3.3 Effects of aging on vulnerability of structures

Even though there has been a substantial increase in interest among researchers in the topic of seismic fragility assessment especially of RC bridges considering aging effects as evidenced by the growing number of published literature (Ghosh and Padgett, 2010 [44]; Castaldo et al., 2017 [21]; Rao et al., 2017 [93]), the fragility analysis of reinforced concrete and masonry structures due to aging effects need to be further investigated. The vulnerability is expected to increase with increasing levels of deterioration since, as already stated, different studies proved that the consideration of aging effects on reinforced concrete structures generally results in resistance, load-bearing capacity and ductility reduction. Explicitly accounting for deterioration requires probabilistic models for predicting the time-dependent level of deterioration of structural elements. In this regard, in the last years, different authors proposed the use of time-dependent seismic fragility functions, i.e. depending on the time of construction, t (Ghosh and Padgett, 2010 [44]; Karapetrou et al., 2013 [59]; Pitilakis et al., 2014 [88]; Castaldo et al., 2017 [21]). The available studies on this topic usually focus on the development of numerical models reflecting different stages of deterioration, comparing the outcomes of the analysis conducted on the initial uncorroded (t = 0 years) and corroded (t = 50 years) concrete structures as shown in Figure 14 (Karapetrou et al., 2013 [59]; Pitilakis et al., 2014 [88]) and on simple SDOF systems (Yalciner et al., 2012 [124]). Besides, the same authors have brought forth the calculation of the rate of erosion, that would allow to evaluate the evolution in the time of fragility.

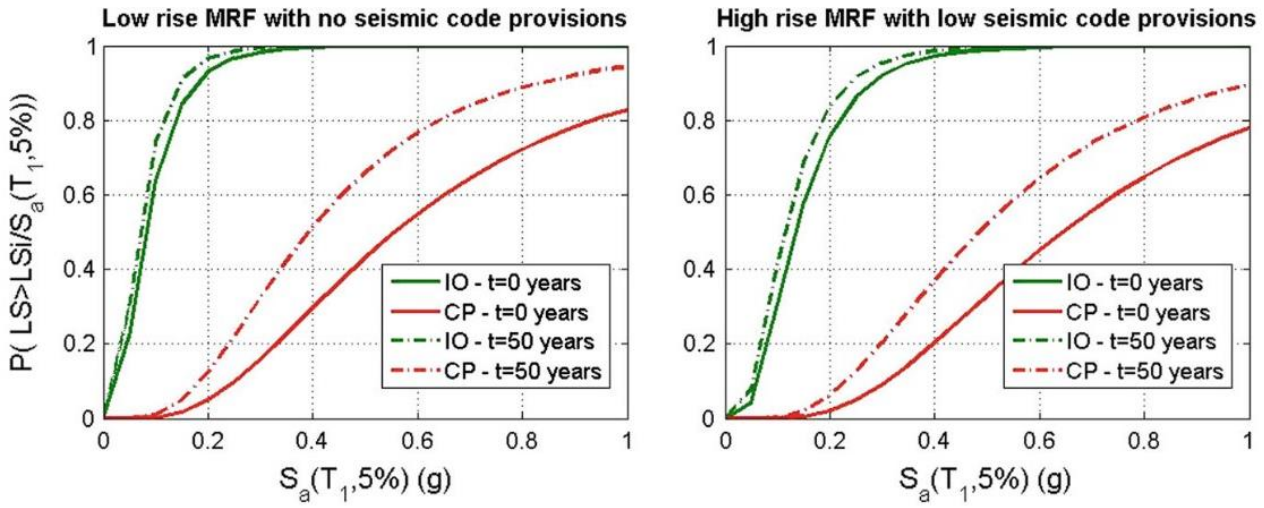

Figure 14 Time dependent fragility curves derived for the initial (t = 0 years) (continuous lines) and corroded (t = 50 years) (dashed lined), for the Immediate occupancy (green line) and collapse prevention (red line) limit states. Considering (a) low-rise and (b) high-rise Moment resistant frame fixed-base buildings from Kappos et al. (2003,2006),[57],[58] in the work of Pitilakis et al. (2014) [88].

Among the several studies carried out for the vulnerability assessment of bridges, Ghosh and Padgett (2010) [44] considered the effect of corrosion on both the demand and capacity models in the evaluation of fragility curves for 4 different damage states, over 100 years. In their study, the progressive and irreversible process caused by aging effects results in an overall increase in structural vulnerability over time. In particular, the median value PGA defining the fragility curve for the complete damage state decreases by 27% after 75 years of exposure to chlorides.

Palazzo et al. (2016) [84] proposed a computational fiber-approach to predict the evolution over time of a deteriorating reinforced concrete element, exposed to an aggressive environment, mainly taking into account deterioration phenomena induced by chlorides attack. The prediction model is based on MonteCarlo simulations in order to define time-variant axial force-bending moment resistance domains. The main findings of this study show a reduction of the reliability index over time, i.e. an increase of the failure probability.

More recently, Rao (2014) [92] developed a model for the fragility assessment including aging effects as a joint function of the ground motion intensity measure, IM, and W the deterioration measure. W represents the time-dependent level of deterioration of a structural component. For example, in the specific case of chloride aging effects induced reinforcement corrosion, W can include the proportion of reinforcement steel mass lost. Stated that seismic capacity and demand are likely to change because of materials' degradation, they will be both dependent on W. This methodology has been applied for the fragility assessment of non-deteriorating and deteriorating columns based on their age and environmental exposure by Rao et al. (2017) [93]. Overall can be seen that the decreasing damage state capacities coupled with increasing seismic demand of older columns lead to fragility functions that increase with increasing deterioration, especially in highly corrosive environments.

Celarec et al. (2011) [24] presented a simplified methodology for seismic performance of aging RC structures considering that the degradation of structural capacity with age can be assumed to follow a power-law relation. Based on an extension of the SAC/FEMA probabilistic framework for estimating mean annual frequencies of limit state exceedance, they presented an analytical solution for equivalent constant limit-state exceedance rates.

Furthermore, Biondini et al. (2011) [13] using lumped plasticity models for seismic analysis of corroded reinforced concrete structures highlighted that consideration of aging effects may lead to a significant reduction of both base shear strength and displacement ductility highlight the importance of a lifetime approach to seismic assessment and design of concrete structures.

More recently, the work of Pitilakis et al. (2014) [88] on the risk assessment of existing RC structures considers among the various aging processes, the chloride-induced corrosion based on probabilistic modelling of corrosion initiation time and corrosion rate. The authors demonstrated that including in the analysis different aging processes as (the loss of reinforcement cross-sectional area, the degradation of concrete cover and the reduction of steel ultimate deformation) may lead to an important shift to the left side of the fragility curves. More in detail, in the case of consideration of aging effects lead to an increase in the probability of damage on the order of 25% for concrete buildings at least 50 years old. In particular, the increase in vulnerability is more pronounced for severe limit-states compared with the ones having a higher probability of occurrence (Karapetrou et al., 2013

2013 [59]). In this light, the same authors propose a more reliable vulnerability assessment performed through time-dependent fragility functions, which can be evaluated taking into account aging effects.

4 Conclusions

This deliverable presents a comprehensive review of the up-to-date literature regarding SFSI and aging effects on the computation of earthquake vulnerability of structures. The main finding is to highlight that studies carried out until now proved that the conventional way of calculating building fragility considering fixed-base and uncorroded structures may lead to a potential underestimation of the seismic risk.

Soil-foundation-structure interaction and local site effects are generally shown to be more pronounced in the case of soft soil formations and high-rise structures, causing considerable modification to the free-field motion, as well as to the dynamic response of the structure. In this light neglecting SFSI and especially site effects may lead to inaccurate fragility and loss estimates, which constitute fundamental components in the risk assessment. Moreover, aging effects on structures might increase their vulnerability and contribute to significant loss of their capacity via a slow, progressive and irreversible process caused by the deterioration of the material properties.

Even though the results of such studies provided the scientific community with valuable knowledge at site-specific vulnerability assessment, the reliability of risk analysis at urban scale is assessed with certain limitations. Further research is necessary for the development of generalized fragility functions applicable to different reinforced concrete and masonry building typologies which would take into account SFSI and site effects for a great variety of soil conditions.

The encouragement in the adoption of reliable SFSI and time-variant models will promote a more accurate assessment of the seismic safety of existing buildings. This aspect is particularly significant in urban risk assessment in order to identify the most appropriate short- and long-term earthquake mitigation policies.

5 References

[1] Argyroudis, S., Tsinidis, G., Gatti, F., Pitilakis, K. (2014). Seismic fragility curves of shallow tunnels considering SSI and aging effects. Proceedings of the 2nd Eastern European Tunnelling Conference, (September), 1–10.

[2] Bakalis, K. and Vamvatsikos, D. (2018) 'Seismic Fragility Functions via Nonlinear Response History Analysis', Journal of Structural Engineering (United States), 144(10). doi: 10.1061/(ASCE)ST.1943-541X.0002141.

[3] Baker, J. W. (2011) 'Conditional mean spectrum: Tool for ground-motion selection', Journal of Structural Engineering, 137(3), pp. 322–331. doi: 10.1061/(ASCE)ST.1943-541X.0000215.

[4] Baker, J. W. and Cornell, C. A. (2006) 'Spectral shape, epsilon and record selection', Earthquake Engineering and Structural Dynamics, 35(9), pp. 1077–1095. doi: 10.1002/eqe.571.

[5] Baker, J. W. (2015) 'Efficient analytical fragility function fitting using dynamic structural analysis' Earthquake Spectra, vol. 31, no. 1, pp. 579–599.

[6] Baltzopoulos, G. et al. (2017) 'SPO2FRAG : software for seismic fragility assessment based on static pushover', Bulletin of Earthquake Engineering, 15(10), pp. 4399–4425. doi: 10.1007/s10518-017-0145-3.

[7] Bazzurro, P. and Cornell, C. A. (1999). Disaggregation of seismic hazard. Bulletin of the Seismological Society of America, 89(2), 501–520.

[8] Behnamfar, F. and Banizadeh, M. (2016) 'Effects of soil-structure interaction on distribution of seismic vulnerability in RC structures', Soil Dynamics and Earthquake Engineering, 80, pp. 73–86. doi: 10.1016/j.soildyn.2015.10.007.

[9] Berto, L., Vitaliani, R., Saetta, A., & Simioni, P. (2009). Seismic assessment of existing RC structures affected by degradation phenomena. Structural Safety, 31(4), 284–297. https://doi.org/10.1016/j.strusafe.2008.09.006

[10] Bianchini, M., Diotallevi, P. P. and Baker, J. W. (2009) 'Prediction of Inelastic Structural Response Using an Average of Spectral Accelerations', p. 8. Available at: http://www.sc.kutc.kansai-u.ac.jp/icossar2009/index.html.

[11] Bindi, D., Pacor, F., Luzi, L., Puglia, R., Massa, M., Ameri, G., & Paolucci, R. (2011). Ground motion prediction equations derived from the Italian strong motion database. Bulletin of Earthquake Engineering, 9(6), 1899–1920. https://doi.org/10.1007/s10518-011-9313-z

[12] Biondini, F. and Vergani, M. (2015) 'Deteriorating beam finite element for nonlinear analysis of concrete structures under corrosion', Structure and Infrastructure Engineering, 11(4), pp. 519–532. doi: 10.1080/15732479.2014.951863.

[13] Biondini, F., Palermo, A. and Toniolo, G. (2011) 'Seismic performance of concrete structures exposed to corrosion: Case studies of low-rise precast buildings', Structure and Infrastructure Engineering, 7(1), pp. 109–119. doi: 10.1080/15732471003588437.

[14] Bradley, B. A., Dhakal, R. P., MacRae, A. G. and Cubrinovski M. (2010) 'Prediction of spatially distributed seismic demands in specific structures: Ground motion and structural response', *Earthq.* Earthquake Engineering & Structural Dynamics, no. 39, pp. 501–520.

[15] Bridges, C. and Betti, R. (1993) 'kinematic soil-structure interaction for long-span', 22(September 1992), pp. 415–430.

[16] BSSC (2004) '2003 Edition NEHRP recommended provisions for seismic regulations for new buildings and other structures (FEMA 450)'.

[17] Calvi, G. M., Pinho, R., Magenes, G., Bommer, J. J., Restrepo-Vélez, L. F., & Crowley, H. (2006). Development of seismic vulnerability assessment methodologies over the past 30 years. ISET Journal of Earthquake Technology, 43(3), 75–104.

[18] Castaldo, P. and Alfano, G. (2020) 'Seismic reliability-based design of hardening and softening structures isolated by double concave sliding devices', Soil Dynamics and Earthquake Engineering, 129(October 2019), p. 105930. doi: 10.1016/j.soildyn.2019.105930.

[19] Castaldo, P., Amendola, G. and Palazzo, B. (2017) 'Seismic fragility and reliability of structures isolated by friction pendulum devices: seismic reliability-based design (SRBD)', Earthquake Engineering and Structural Dynamics, 46(3), pp. 425–446. doi: 10.1002/eqe.2798.

[20] Castaldo, P., Palazzo, B. and Ferrentino, T. (2017) 'Seismic reliability-based ductility demand evaluation for inelastic base-isolated structures with friction pendulum devices', Earthquake Engineering and Structural Dynamics, 46(8), pp.

1245–1266. doi: 10.1002/eqe.2854.

[21] Castaldo, P., Palazzo, B. and Mariniello, A. (2017) 'Effects of the axial force eccentricity on the time-variant structural reliability of aging r. c. cross-sections subjected to chloride-induced corrosion', Engineering Structures, 130, pp. 261–274. doi: 10.1016/j.engstruct.2016.10.053.

[22] Cavalieri, F., Correia, A. A., Crowley, H., & Pinho, R. (2020). Dynamic soil-structure interaction models for fragility characterisation of buildings with shallow foundations. Soil Dynamics and Earthquake Engineering, 132(December 2019). https://doi.org/10.1016/j.soildyn.2019.106004

[23] CEB-FIB Task Group 5.6 (2006) Model for service life design, fédération internationale du béton (fib).

[24] Celarec, D., Vamvatsikos, D., & Dolšek, M. (2011). Simplified estimation of seismic risk for reinforced concrete buildings with consideration of corrosion over time. Bulletin of Earthquake Engineering, 9(4), 1137–1155. https://doi.org/10.1007/s10518-010-9241-3

[25] Ciampoli, M. and Pinto, P. E. (1995) 'Effects of soil-structure interaction on inelastic seismic response of bridge piers', Journal of Structural Engineering (United States), 121(5), pp. 806–814. doi: 10.1061/(ASCE)0733-9445(1995)121:5(806).

[26] Cornell, C. A., Asce, M., Jalayer, F., Hamburger, R. O., Asce, M., Foutch, D. A., & Asce, M. (2002). Management Agency Steel Moment Frame Guidelines. 128(4), 526–533.

[27] Coronelli, D. and Gambarova, P. (2004) 'Structural Assessment of Corroded Reinforced Concrete Beams: Modeling Guidelines', Journal of Structural Engineering, 130(8), pp. 1214–1224. doi: 10.1061/(ASCE)0733-9445(2004)130.

[28] Cosenza, E., Manfredi, G. and Pecce, M. (2008) Strutture in cemento armato – basi della progettazione. HOEPLI: Milan, Italy. Available at: https://iris.unisannio.it/handle/20.500.12070/14190#.X5r3ZYhKg2w.

[29] Crowley, H., Polidoro, B., Pinho, R. and J. Van Elk, (2017) 'Framework for developing fragility and consequence models for local personal risk', *Earthq. Spectra*, vol. 33, no. 4, pp. 1325–1345.

[30] D'Ayala D, Meslem A, Vamvatsikos D, Porter K, Rossetto T, Crowley H and Silva V (2013) Guidelines for analytical vulnerability assessment: Low/mid-rise. GEM technical report 8. Avaiable at: globalquakemodel.org. doi 10.13117/GEM.VULN-MOD.TR2014.12

[31] De Risi, R., Penna, A. and Simonelli, A. L. (2019) 'Seismic risk at urban scale: the role of site response analysis', Soil Dynamics and Earthquake Engineering, 123(February), pp. 320–336. doi: 10.1016/j.soildyn.2019.04.011.

[32] de Silva, F. (2020) 'Influence of soil-structure interaction on the site-specific seismic demand to masonry towers', Soil Dynamics and Earthquake Engineering, 131(January), p. 106023. doi: 10.1016/j.soildyn.2019.106023.

[33] de Silva, F., Ceroni, F., Sica, S., Pecce, M. R., & Silvestri, F. (2015). Effects of soil-foundation-structure interaction on the seismic behavior of monumental towers: The case study of the Carmine Bell Tower in Naples. Rivista Italiana Di Geotecnica, 49(3), 7–27.

[34] DuraCrete (1998) Modelling of degradation, EU-project (Brite EuRam III) no. BE95-1347. Probabilistic performance based durability design of concrete structures. Report 4–5;

[35] Dutta, S. C., Bhattacharya, K. and Roy, R. (2004) 'Response of low-rise buildings under seismic ground excitation incorporating soil-structure interaction', Soil Dynamics and Earthquake Engineering, 24(12), pp. 893–914. doi: 10.1016/j.soildyn.2004.07.001.

[36] Eads, L., Ribeiro, F. and Barbosa, A. (2013) 'Dynamic analysis of 2-Story moment frame', Stanford University, pp. 2–5. Available at: http://opensees.berkeley.edu/wiki/index.php/Dynamic_Analysis_of_2-Story_Moment_Frame.

[37] Ebrahimian, H., Jalayer, F., Lucchini, A., Mollaioli, F., & Manfredi, G. (2015). Preliminary ranking of alternative scalar and vector intensity measures of ground shaking. Bulletin of Earthquake Engineering, 13(10), 2805–2840. https://doi.org/10.1007/s10518-015-9755-9

[38] Ellingwood, B. R. and Kinali, K. (2009) 'Quantifying and communicating uncertainty in seismic risk assessment', Structural Safety, 31(2), pp. 179–187. doi: 10.1016/j.strusafe.2008.06.001.

[39] Elsabee, F. and Murray, J. P. (1977) 'Dynamic Behavior of Embedded Foundations', R77-33, (578), pp. 5–6.

[40] Fathi, A., Sadeghi, A., Emami Azadi, M. R., & Hoveidae, N. (2020). Assessing the soil-structure interaction effects by direct method on the out-of-plane behavior of masonry structures (case study: Arge-Tabriz). Bulletin of Earthquake Engineering, 18(14), 6429–6443. https://doi.org/10.1007/s10518-020-00933-w

[41] FEMA-NIBS (2004) Multi-hazard loss estimation methodology: Earthquake model: HAZUS MH technical manual. Technical report, Pacific Earthquake Engineering Research Center, Washington, DC.
[42] Gazetas, G. (1983) 'Analysis of machine foundation vibrations: State of the art', International Journal of Soil Dynamics and Earthquake Engineering, 2(1), pp. 2–42. doi: 10.1016/0261-7277(83)90025-6.
[43] Gazetas, G. (1991) 'Formulas and charts for impedances of surface and embedded foundations', 117(9).
[44] Ghosh, J. and Padgett, J. E. (2010) 'Aging considerations in the development of time-dependent seismic fragility curves', Journal of Structural Engineering, 136(12), pp. 1497–1511. doi: 10.1061/(ASCE)ST.1943-541X.0000260.
[45] Giovenale, P., Cornell, C. A. and Esteva, L. (2004) 'Comparing the adequacy of alternative ground motion intensity measures for the estimation of structural responses', Earthquake Engineering and Structural Dynamics, 33(8), pp. 951–979. doi: 10.1002/eqe.386.
[46] Güllü, H. and Jaf, H. S. (2016) 'Full 3D nonlinear time history analysis of dynamic soil–structure interaction for a historical masonry arch bridge', Environmental Earth Sciences, 75(21). doi: 10.1007/s12665-016-6230-0.
[47] Harden, C., Hutchinson, T. and Martin, G. R. (2005) 'Numerical Modeling of the Nonlinear Cyclic Response of Shallow Foundations', Pacific Earthquake Engineering Research Center.
[48] Iervolino, I. and Cornell, C. A. (2005) 'Record selection for nonlinear seismic analysis of structures', Earthquake Spectra, 21(3), pp. 685–713. doi: 10.1193/1.1990199.
[49] INGV- Istituto Nazionale di Geofisica e Vulcanologia. Dati online della pericolosità sismica. Available at: http://esse1.mi.ingv.it/.
[50] Jalayer, F. and Allin Cornell, C. (2009) 'Alternative non-linear demand estimation methods for probability-based seismic assessments', Earthquake Engineering and Structural Dynamics, (38), pp. 951–972. doi: 10.1002/eqe.
[51] Jalayer, F., Cornell, C. A. and Cornell, C. A. (2003) 'A Technical Framework for Probability-Based Demand and Capacity Factor Design (DCFD) Seismic Formats A Technical Framework for Probability-Based Demand and Capacity Factor Design (DCFD) Seismic Formats'.
[52] Jalayer, F., De Risi, R. and Manfredi, G. (2015) 'Bayesian Cloud Analysis: Efficient

structural fragility assessment using linear regression', Bulletin of Earthquake Engineering, 13(4), pp. 1183–1203. doi: 10.1007/s10518-014-9692-z.

[53] Jalayer, F., Ebrahimian, H., Miano, A., Manfredi, G., & Sezen, H. (2017). Analytical fragility assessment using unscaled ground motion records. Earthquake Engineering and Structural Dynamics, 46(15), 2639–2663. https://doi.org/10.1002/eqe.2922

[54] Jayaram, N., Lin, T. and Baker, J. W. (2011) 'A Computationally efficient ground-motion selection algorithm for matching a target response spectrum mean and variance', Earthquake Spectra, 27(3), pp. 797–815. doi: 10.1193/1.3608002.

[55] Kappos, A. J. (2016) 'An overview of the development of the hybrid method for seismic vulnerability assessment of buildings', Structure and Infrastructure Engineering, 12(12), pp. 1573–1584. doi: 10.1080/15732479.2016.1151448.

[56] Kappos, A. J., Panagiotopoulos, C. and Panagopoulos, G. (2004) 'Derivation of fragility curves using inelastic time-history analysis and damage statistics', Icces'04, pp. 665–672.

[57] Kappos, A. J., Panagiotopoulos, C., Panagopoulos, G., & Papadopoulos, E. (2003). WP4 – REINFORCED CONCRETE BUILDINGS (Level I and II analysis).

[58] Kappos, A. J., Panagopoulos, G., Panagiotopoulos, C., Penelis, G. (2006). "A Hybrid Method for the Vulnerability Assessment of R/C and URM Buildings." Bulletin of Earthquake Engineering 4 (4): 391–413. https://doi.org/10.1007/s10518-006-9023-0.

[59] Karapetrou, S. T., Filippa, A. M., Fotopoulou, S. D., & Pitilakis, K. D. (2013). Time-dependent vulnerability assessment of RC buildings considering SSI and aging effects. ECCOMAS Thematic Conference - COMPDYN 2013: 4th International Conference on Computational Methods in Structural Dynamics and Earthquake Engineering, Proceedings - An IACM Special Interest Conference, (June), 4117–4134.

[60] Karapetrou, S. T., Fotopoulou, S. D. and Pitilakis, K. D. (2015) 'Seismic vulnerability assessment of high-rise non-ductile RC buildings considering soil-structure interaction effects', Soil Dynamics and Earthquake Engineering, 73, pp. 42–57. doi: 10.1016/j.soildyn.2015.02.016.

[61] Karatzetzou, A., Pitilakis, D. and Stefanidou, S. (2020) 'Partitioning Displacement Demand of Flexible-base Structures because of SSI', Journal of Earthquake Engineering, 00(00), pp. 1–18. doi: 10.1080/13632469.2020.1772149.

[62] Karatzetzou, A., Pitilakis, D., Kržan, M., & Bosiljkov, V. (2015). Soil–foundation–structure interaction and vulnerability assessment of the Neoclassical School in Rhodes, Greece. Bulletin of Earthquake Engineering, 13(1), 411–428. https://doi.org/10.1007/s10518-014-9637-6

[63] Karatzetzou, A., Riga, E., & Pitilakis, K. (2017). Urban-scale soil-structure interaction effects for risk assessment : the case of Thessaloniki city, Greece.

[64] Kiureghian, A. Der and Ditlevsen, O. (2009) 'Aleatory or epistemic? Does it matter?', Structural Safety, 31(2), pp. 105–112. doi: 10.1016/j.strusafe.2008.06.020.

[65] Kohrangi, M., Vamvatsikos, D., & Bazzuro, P. (2018). The role of spectral shape and pulse period for record selection in the near field. Eleventh U.S. National Conference on Earthquake Engineering, (June).

[66] Kramer, S. L. (1996) Geotechnical EARTHQUAKE engineering. Prentice Hall Series.

[67] Kutanis, M. and Elmas, M. (2001) 'Non-Linear Seismic Soil-Structure Interaction Analysis Based on Sismik Y ¨ sımı C', Turk J Engin Environ Sci, 25, pp. 617–626.

[68] Lagomarsino, S. and Cattari, S. (2015) 'PERPETUATE guidelines for seismic performance-based assessment of cultural heritage masonry structures', Bulletin of Earthquake Engineering, 13(1), pp. 13–47. doi: 10.1007/s10518-014-9674-1.

[69] Lin, T., Haselton, C. B. and Baker, J. W. (2013a) 'Conditional spectrum-based ground motion selection . Part I : Hazard consistency for risk-based assessments', (June), pp. 1847–1865. doi: 10.1002/eqe.

[70] Lin, T., Haselton, C. B. and Baker, J. W. (2013b) 'Conditional spectrum-based ground motion selection . Part II : Intensity-based assessments and evaluation of alternative target spectra', (May), pp. 1867–1884. doi: 10.1002/eqe.

[71] Luco, N. and Cornell, C. A. (2007) 'Structure-specific scalar intensity measures for near-source and ordinary earthquake ground motions', Earthquake Spectra, 23(2), pp. 357–392. doi: 10.1193/1.2723158.

[72] Maravas, A., Mylonakis, G. and Karabalis, D. L. (2014) 'Simplified discrete systems for dynamic analysis of structures on footings and piles', Soil Dynamics and Earthquake Engineering, 61–62(May), pp. 29–39. doi: 10.1016/j.soildyn.2014.01.016.

[73] Martins L. and Silva V. 'Development of a fragility and vulnerability model for global seismic risk analyses' (2020), *Bulletin of Earthquake Engineering.*

https://doi.org/10.1007/s10518-020-00885-1

[74] Mazzoni, S., Mckenna, F., Scott, M. H., & Fenves, G. L. (2006). The Open System for Earthquake Engineering Simulation (OpenSEES) User Command-Language Manual. Retrieved from http://citeseerx.ist.psu.edu/viewdoc/summary?doi=10.1.1.476.1843

[75] Michel, C. & Guéguen, P. (2012). Seismic vulnerability assessment based on vibration data at the city-scale. 15th World Conference on Earthquake Engineering (15WCEE), (July), 2–9.

[76] Mitropoulou, C. C., Kostopanagiotis, C., Kopanos, M., Ioakim, D., & Lagaros, N. D. (2016). Influence of soil-structure interaction on fragility assessment of building structures. Structures, 6, 85–98. https://doi.org/10.1016/j.istruc.2016.02.005

[77] Mylonakis, G. and Gazetas, G. (2000) 'Seismic soil-structure interaction: Beneficial or detrimental?', Journal of Earthquake Engineering, 4(3), pp. 277–301. doi: 10.1080/13632460009350372.

[78] Mylonakis, G., Nikolaou, S. and Gazetas, G. (2006) 'Footings under seismic loading: Analysis and design issues with emphasis on bridge foundations', Soil Dynamics and Earthquake Engineering, 26(9), pp. 824–853. doi: 10.1016/j.soildyn.2005.12.005.

[79] Nakhaei, M. and Ali Ghannad, M. (2008) 'The effect of soil-structure interaction on damage index of buildings', Engineering Structures, 30(6), pp. 1491–1499. doi: 10.1016/j.engstruct.2007.04.009.

[80] NIST (2012) Soil-structure interaction for building structures. Technical report, US Department of Commerce, Washington, DC.

[81] Pais, A. and Kausel, E. (1988) 'Approximate formulas for dynamic stiffnesses of rigid foundations', Soil Dynamics and Earthquake Engineering, 7(4), pp. 213–227. doi: 10.1016/S0267-7261(88)80005-8.

[82] Paolucci, R. (1993). Soil-structure interaction effects on an instrumented building in Mexico City. European Earthquake Engineering, 3. https://doi.org/10.1007/s10518-007-9042-5.

[83] Paolucci, R., Figini, R., & Petrini, L. (2013). Introducing dynamic nonlinear soil-foundation-structure interaction effects in displacement-based seismic design. Earthquake Spectra, 29(2), 475–496. https://doi.org/10.1193/1.4000135

[84] Palazzo, B., Castaldo, P. and Mariniello, A. (2016) 'Time-Variant Reliability of RC Structures', Applied Mechanics and Materials, 847, pp. 407–414. doi:

10.4028/www.scientific.net/amm.847.407.

[85] Petridis, C. and Pitilakis, D. (2020) 'Fragility curve modifiers for reinforced concrete dual buildings, including nonlinear site effects and soil–structure interaction', Earthquake Spectra, (June 2019). doi: 10.1177/8755293020919430.

[86] Piro, A., de Silva, F., Parisi, F., Scotto di Santolo, A., & Silvestri, F. (2020). Effects of soil-foundation-structure interaction on fundamental frequency and radiation damping ratio of historical masonry building sub-structures. Bulletin of Earthquake Engineering, 18(4), 1187–1212. https://doi.org/10.1007/s10518-019-00748-4.

[87] Pitilakis, D., Moderessi-Farahmand-Razavi, A., & Clouteau, D. (2013). Equivalent-linear dynamic impedance functions of surface foundations. Journal of Geotechnical and Geoenvironmental Engineering, 139(7), 1130–1139. https://doi.org/10.1061/(ASCE)GT.1943-5606.0000829.

[88] Pitilakis, K. D., Karapetrou, S. T. and Fotopoulou, S. D. (2014) 'Consideration of aging and SSI effects on seismic vulnerability assessment of RC buildings', Bulletin of Earthquake Engineering, 12(4), pp. 1755–1776. doi: 10.1007/s10518-013-9575-8.

[89] Pitilakis, K., Crowley, H. and Kaynia, A. M. (2014) SYNER-G: Typology Definition and Fragility Functions for Physical Elements at Seismic Risk, 11. Available at: http://link.springer.com/10.1007/978-94-007-7872-6.

[90] Porter, K., Kennedy, R. and Bachman, R. (2007) 'Creating fragility functions for performance-based earthquake engineering', Earthquake Spectra, 23(2), pp. 471–489. doi: 10.1193/1.2720892.

[91] Rajeev, P. and Tesfamariam, S. (2012) 'Seismic fragilities of non-ductile reinforced concrete frames with consideration of soil structure interaction', Soil Dynamics and Earthquake Engineering, 40, pp. 78–86. doi: 10.1016/j.soildyn.2012.04.008.

[92] Rao, A. S. (2014) Structural Deterioration and Time Dependent Seismic Risk Analysis. Department of Civil and Environmental Engineering. Stanford University, Stanford, CA, USA. Available at: https://purl.stanford.edu/ss552fb7739.

[93] Rao, A. S., Lepech, M. D. and Kiremidjian, A. (2017) 'Development of time-dependent fragility functions for deteriorating reinforced concrete bridge piers1', Structure and Infrastructure Engineering, 13(1), pp. 67–83. doi: 10.1080/15732479.2016.1198401.

[94] Rao, A. S., Lepech, M. D., Kiremidjian, A. S., & Sun, X. Y. (2017). Simplified structural deterioration model for reinforced concrete bridge piers under cyclic

loading1. Structure and Infrastructure Engineering, 13(1), 55–66. https://doi.org/10.1080/15732479.2016.1198402.

[95] Raychowdhury, P.; Hutchinson, T. C. (2008) 'ShallowFoundationGen OpenSees Documentation', Tara, pp. 1–26.

[96] Riga, E., Karatzetzou, A., Fotopoulou, S., & Dafloukas, K. (2019). Urban seismic risk model for resilient cities . The case of Thessaloniki. (October).

[97] Riga, E., Karatzetzou, A., Mara, A., & Pitilakis, K. (2017). Studying the uncertainties in the seismic risk assessment at urban scale applying the Capacity Spectrum Method: The case of Thessaloniki. Soil Dynamics and Earthquake Engineering, 92(September 2016), 9–24. https://doi.org/10.1016/j.soildyn.2016.09.043.

[98] Rodriguez, J. and Geocısa, C. A.- (2001) 'CONTECVET A validated users manual for assessing the residual service life of concrete structures'.

[99] Rossetto, T. and Elnashai, A. (2003) 'Derivation of vulnerability functions for European-type RC structures based on observational data', Engineering Structures, 25(10), pp. 1241–1263. doi: 10.1016/S0141-0296(03)00060-9.

[100] Rovithis, E., Makra, K., Savvaidis, A., Karakostas, C., & Lekidis, V. (2016). Airborne LiDAR and field data combination towards SSI applications at large- scale : The case of the Kalochori urban area in Greece Airborne LiDAR and field data combination towards SSI applications at large-scale : The case of the Kalochori urban area in. (July).

[101] Sabetta, F., & Pugliese, A. (1987). Attenuation Of Peak Horizontal Acceleration And Velocity From Italian Strong-Motion Records. Bulletin of the Seismological Society of America, 77(5).

[102] Sabetta, F., Goretti, A. and Lucantoni, A. (1998). 'Empirical Fragility Curves from Damage Surveys and Estimated Strong Ground Motion', 11th European Conference on Earthquake Engineering, (May 2014), pp. 1–11.

[103] Saetta, A., Scotta, R. and Vitaliani, R. (1999). 'Coupled Environmental-Mechanical Damage Model Of Rc Structures', journal of engineering mechanics, 125(8), pp. 930–940.

[104] Saetta, A., Simioni, P., Berto, L., & Vitaliani, R. (2008). Seismic response of corroded r.c. structures. Proceedings of the International FIB Symposium 2008 - Tailor Made Concrete Structures: New Solutions for Our Society, 228. https://doi.org/10.1201/9781439828410.ch167.

[105] Sáez, E., Lopez-Caballero, F. and Modaressi-Farahmand-Razavi, A. (2011) 'Effect of the inelastic dynamic soil-structure interaction on the seismic vulnerability assessment', Structural Safety, 33(1), pp. 51–63. doi: 10.1016/j.strusafe.2010.05.004.

[106] Shinozuka, M., Feng, M. Q., Lee, J., & Naganuma, T. (2000). Statistical Analysis Of Fragility Curves. Journal Of Engineering Mechanics /, 126(December), 1224–1231..

[107] Shome, N., Cornell, C. A., M.EERI, Bazzurro, P., & J., Carballo. (1998). Earthquakes, Records and Nonlinear Responses.pdf.

[108] Shome, Nilesh, and Carl Allin Cornell. 2000. "Structural Seismic Demand Analysis: Consideration of Collapse." 8th ACSE Specialty Conference on Probabilistic Mechanics and Structural Reliability, no. 3: PMC2000-119. http://www.rms-group.org/rms_papers/pdf/nilesh/pmc.pdf.

[109] Silva, V., Baker, J. W., Bazzurro, P., Vamvatsikos, D., & Pitilakis, K. (2019). Current challanges and future trends in analytical fragility and vulnerability modelling. Earthquake Spectra (PREPRINT), 1–33. https://doi.org/10.1016/j.ssresearch.2016.09.015.

[110] Smerzini, C., & Pitilakis, K. (2018). Seismic risk assessment at urban scale from 3D physics-based numerical modeling: the case of Thessaloniki. Bulletin of Earthquake Engineering, 16(7), 2609–2631. https://doi.org/10.1007/s10518-017-0287-3.

[111] Stafford P.J. (2008). Conditional prediction of absolute durations. Bulletin of Seismological Society of America, 98(3), pp. 1588-1594.

[112] Stewart, B. J. P., Seed, R. B. and Fenves, G. L. (1999) 'Seismic soil-structure interaction in buildings. I: Analytical aspects', J. Geotech. & Geoenv. Engrg., (January), pp. 38–48.

[113] Stewart, J. P., Seed, R. B. and Fenves, G. L. (1999) 'Seismic soil-structure interaction in buildings. II: Empirical findings', J. Geotech. & Geoenv. Engrg.

[114] Tomeo, R., Pitilakis, D., Bilotta, A., & Nigro, E. (2018). SSI effects on seismic demand of reinforced concrete moment resisting frames. Engineering Structures. https://doi.org/10.1016/j.engstruct.2018.06.104.

[115] Tothong, P. and Luco, N. (2007) 'Probabilistic seismic demand analysis using advanced ground motion intensity measures', Earthquake Engineering and Structural Dynamics, (36), pp. 1837–1860. doi: 10.1002/eqe.

[116] Tuutti, K. (1982) Corrosion of steel in concrete. Stockholm, Sweden. Available at: https://www.diva-portal.org/smash/record.jsf?pid=diva2%3A960656&dswid=9779 (Accessed: 29 October 2020).
[117] U.S. Geological Survey. Seismic Hazard Maps and Site-Specific Data. Available at: https://www.usgs.gov/natural-hazards/earthquake-hazards/seismic-hazard-maps-and-site-specific-data (Accessed: 30 October 2020).
[118] Vamvatsikos, D. and Allin Cornell, C. (2002) 'Incremental dynamic analysis', Earthquake Engineering and Structural Dynamics, 31(3), pp. 491–514. doi: 10.1002/eqe.141.
[119] Vamvatsikos, D., Jalayer, F., & Cornell, C. A. (2003). Application Of Incremental Dynamic Analysis To An Rc-Structure. Proceedings Of The Fib Symposium on Concrete Structures in Seismic Regions., (Figure 1), 1–12.
[120] Veletsos, A. S. and Damodaran Nair, V. V. (1974) 'Torsional Vibration of Viscoelastic Foundations.', ASCE J Geotech Eng Div, 100(GT3), pp. 225–246. doi: 10.1016/0148-9062(74)91893-2.
[121] Veletsos, A. S. and Meek, J. W. (1974) 'Dynamic behaviour of building-foundation systems', Earthquake Engineering & Structural Dynamics, 3(2), pp. 121–138. doi: 10.1002/eqe.4290030203.
[122] Vidic, T., Fajfar, P., Fischinge M. (1994) 'Consistent inelastic design spectra: Hysteretic and input energy', Earthquake Engineering & Structural Dynamics, 23(5), pp. 523–537. doi: 10.1002/eqe.4290230505.
[123] Wolf, J. P. (1985) 'Dynamic soil-structure interaction.', Dynamic soil-structure interaction.
[124] Yalciner, H., Sensoy, S. and Eren, O. (2012) 'Time-dependent seismic performance assessment of a single-degree-of-freedom frame subject to corrosion', Engineering Failure Analysis, 19(1), pp. 109–122. doi: 10.1016/j.engfailanal.2011.09.010.